

Title: Symbiotic bacterial network structure involved in carbon and nitrogen metabolism of wood-utilizing insect larvae.

Running head: wood utilization and insect bacterial symbionts

Authors: Hirokuni Miyamoto*^{1,2,3,4}, Futo Asano¹, Koutarou Ishizawa⁵, Wataru Suda², Hisashi Miyamoto⁶, Naoko Tsuji³, Makiko Matsuura^{1,3}, Arisa Tsuboi^{3,4,7}, Chitose Ishii^{1,2,3}, Teruno Nakaguma^{1,3,4}, Chie Shindo², Tamotsu Kato², Atsushi Kurotani⁷, Hideaki Shima⁷, Shigeharu Moriya^{1,7}, Masahira Hattori^{2,8}, Hiroaki Kodama¹, Hiroshi Ohno², Jun Kikuchi*⁷

Affiliations:

1. Graduate School of Horticulture, Chiba University, Matsudo, Chiba 271-8501, Japan
2. RIKEN IMS, Yokohama, Kanagawa 230-0045, Japan
3. Sermas Co., Ltd., Ichikawa, Chiba 272-0033, Japan
4. Japan Eco-science (Nikkan Kagaku) Co. Ltd., Chiba, Chiba 260-0034, Japan
5. Elementary School of Batou, Nakagawa, Tochigi 324-0613, Japan
6. Miroku Co., Ltd., Kitsuki, Oita 873-0021, Japan
7. RIKEN CSRS, Yokohama, Kanagawa 230-0045, Japan
8. School of Advanced Science and Engineering, Waseda University, Tokyo 169-8555, Japan

* Co-corresponding authors

Correspondence: Hirokuni Miyamoto Ph.D., Chiba University, RIKEN, Sermas Co., Ltd. and Japan Eco-science Co., Ltd.

Tel: +81-43-290-3947, Fax: +81-43-290-3947

E-mail: hirokuni.miyamoto@riken.jp, h-miyamoto@faculty.chiba-u.jp

Correspondence: Jun Kikuchi Ph.D., RIKEN

Tel: +81-43-290-3942, Fax: +81-43-290-3942

E-mail: jun.kikuchi@riken.jp

Abstract

Effective biological utilization of wood biomass is necessary worldwide. Since several insect larvae can use wood biomass as a nutrient source, studies on their digestive mechanism are expected to speculate a novel rule in wood biomass processing. Here, the relationships of inhabitant bacteria involved in carbon and nitrogen metabolism in the intestine of beetle larvae, an insect model, are investigated. Bacterial analysis of larval feces showed enrichment of the phyla Chroloflexi, Gemmatimonadetes, and Plactomysetes and genera *Bradyrhizobium*, *Chonella*, *Corallococcus*, *Gemmata*, *Hyphomicrobium*, *Lutibacterium*, *Paenibacillus*, and *Rhodoplanes*, members of which could include candidates for plant growth promotion, nitrogen cycle modulation, and/or environmental protection. The abundances of these bacteria were not necessarily positively correlated with the abundance in the habitat, suggesting that they might be selectively enriched in the intestines of larvae. Further association analysis predicted that carbon and nitrogen metabolism in the intestine was affected by the presence of the other common bacteria, *i.e.* phyla Acidobacteria, Armatimonadetes, and Bacteroidetes and genera *Candidatus Solibacter*, *Devosia*, *Fimbrimonas*, *Gemmatimonas*, *Pilimelia*, *Sphingomonas*, and *Methanobacterium*, the populations of which were not remarkably altered in the habitat and feces. Based on hypotheses targeting these selected bacterial

groups, structural estimation modeling analyses statistically suggested that their metabolism of carbon and nitrogen and their stable isotopes, $\delta^{13}\text{C}$ and $\delta^{15}\text{N}$, may be associated with fecal enriched bacteria and other common bacteria. In addition, other causal inference analyses, such as causal mediation analysis, linear non-Gaussian acyclic model (LiNGAM), and BayesLiNGAM, did not necessarily affirm the existence of prominent bacteria involved in metabolism, implying its importance as the bacterial groups for metabolism rather than a remarkable bacterium. Thus, these observations highlight a multifaceted view of symbiotic bacterial groups utilizing carbon and nitrogen from wood biomass in insect larvae as a cultivator of potentially environmentally beneficial bacteria. (292/300words)

Keywords: Beetle/Wood biomass/Symbiosis

Abbreviations: anammox, anaerobic ammonium oxidization; SDGs, sustainable development goals

Introduction

Although insects are the most abundant organisms worldwide and constitute more than 50% of all known animal species, the biodiversity of insects is threatened, and dramatic

rates of decline are predicted ¹⁻⁵. Since insects play various roles in the ecosystem ⁶⁻¹⁴ and their importance is evident, many studies on planetary boundaries ¹⁵ and sustainable development goals (SDGs) are required ¹⁶. With the increasing need to meet SDGs, the protection of woody biomass is also an urgent issue. Insects coexist by utilizing wood biomass as feed and habitat. Since thinning of wood is essential for the protection of forests ¹⁷, efficient wood recycling by using insects is expected to protect insects and forests by enhancing their capabilities.

Possible applications for efficient recycling of wood include the use of wood components themselves as a raw material for biomass energy and the use of insects, which can be cultivated by using wood as feed, for various applications¹⁸⁻²³, *e.g.*, for decomposition of wood-derived cellulose to sugar for the production of bioethanol ²⁴, as protein sources within the feed of industrial animals ²⁵, and as feed additives²⁶ to improve the feed conversion ratio of livestock animals to utilize cellulose within the feed. To realize this goal, it is necessary to understand the symbiotic microorganisms associated with digestion in insects. Research on the significance of symbioses between insects, more phylogenetically broader arthropod taxa, and their symbiotic microorganisms for the utilization of wood biomass residues has been performed under various research viewpoints ²⁷⁻³⁷. As the most abundant organisms worldwide, insects may play multiple

essential roles in ecosystems. Therefore, studies that aim to understand the potential application of gut microbes in the medical, engineering, and industrial fields and the protection of ecosystems^{38,39} are becoming increasingly necessary.

As a first step toward these goals, the bacterial community in larvae of the Japanese rhinoceros beetle (*Trypoxylus dichotomus*), an insect model that utilizes wood, is analyzed here. The symbiotic relationship between environmentally beneficial bacterial candidates in the habitat of beetle larvae and their excreted feces was predicted by correlation and association analysis together with carbon and nitrogen metabolism (Fig. 1). The structural equation model was constructed from the hypothesis set based on these data. Furthermore, causal mediation analysis, LiNGAM, and BayesLiNGAM estimated the importance of microbial groups for the metabolism of carbon and nitrogen and their stable isotopes. These observations will enable speculation on the systemic relationships of microbes and inference of the role of beetle larvae as a potential grower of environmentally beneficial bacterial candidates from wood biomass. The findings are expected to provide a crucial viewpoint as an essential viewpoint that will lead to the conservation of nature strongly related to insects as well as the innovation of environmental industries in the future.

Materials and Methods

Sample preparation

Japanese rhinoceros beetles (*T. dichotomus*) living in a forest in Japan (E140°10'N36°75') were collected, and thereafter, they were subcultured and naturally mated within the same box (box size: length 33.5 cm x width 49.0 cm x height 31.0 cm) with wood chips (Kunugi mat, Daiso Co., Ltd.) as the habitat. The larvae were subcultured in the same box, which was covered to prevent adults from flying, and wood chips were randomly added. After that, mating was repeated from 2015 until 2018. Then, in May 2018, male and female larvae were transferred to the same small box (box size: vertical 13.0 cm x horizontal 21.0 cm x height 13.5 cm), and fresh wood chips were placed in the box (n=2, male is n=1 and female is n=1, per box). Since an appropriate water concentration on wood chips is necessary for the habitat of beetle larvae, water should be moderately sprayed. To evaluate the effects of the environmental bacteria, the six boxes were prepared and divided into two groups as follows (Table S1): 1) normally managed group I (three boxes) with spraying tap water; 2) group II (three boxes) managed with spraying tap water containing an environmental bacterial solution, an extract of compost with thermophilic Bacillaceae⁴⁰⁻⁴⁵. The extract was adjusted to 20% as the total volume of tap water. Water was sprayed *ad libitum* according to the degree of moisture in the wood chips.

However, the timing and number of sprays for Group I and Group II were the same. Fresh wood chips were added once every two weeks, and the decayed chips (similar to soil) and feces were collected after 4 weeks. Wood chips, decayed chips (M-chips, as indicated in the figures and tables), and feces were used for analyses in this study.

Bacterial community analysis

DNA from the decayed chips and feces was isolated using a QIAGEN QIAamp PowerFecal DNA Kit according to the manufacturer's protocol (QIAGEN, USA). The DNA concentrations were evaluated using the Quant-iT™ PicoGreen dsDNA Assay Kit (Thermo Fisher Scientific, USA). The V4 region (515F-806R) of the bacterial 16S rRNA gene was sequenced on an Illumina MiSeq according to a previous study^{46,47}. The obtained sequences were filtered by Trimmomatic (<http://www.usadellab.org/cms/?page=trimmomatic>). The trimmed 10,000 reads per sample were analyzed with QIIME 1.9.1 as previously described⁴⁸. The filtered sequences were clustered into operational taxonomic units (OTUs), which were defined at 97% similarity. The α -diversity, β -diversity, bacterial community, and correlation heatmap were visualized by using the packages “genefilter”, “gplots”, “ggplot2”, “RColorBrewer”, “pheatmap”, “ape”, “base”, “dplyr”, “easyGgplot2”, “knitr”, “ggthemes”, “phyloseq”,

and “vegan” in R software (version 3.6.2 and 4.0.5) ^{49,50}, Microsoft 365, and Prism software (version 9.1.0). The number of observed OTUs and the values of Chao1, Shannon, and Simpson, as α -diversity, were assessed. The β -diversities were estimated by principal coordinate analysis (PCoA) using weighted or unweighted UniFrac distances based on the OTU distribution across samples. Relative abundances of bacterial populations of phyla and genera were selected from the majority (> 1% of the detected population) and represented. The Unifrac distances were analyzed by adonis in the packages “vegan” and “MASS” of R software, and alpha diversity graphs and Unifrac graphs were also prepared by using R software ^{49,51}. The relative abundances of individual phyla and genera categorized without discrimination of OTUs were compared within the major community (comparison in >1% of the total bacterial community). The bacterial community was analyzed by paired t-test and Mann–Whitney U test/Wilcoxon sign-rank tests, as appropriate, and the estimation plots were prepared by using Prism software. The relative values of dominant and/or characteristic bacteria were visualized through the construction of a correlation heatmap after the Pearson correlation coefficient was calculated for the selected bacteria (> 1% of the detected community) by using R software. Bacteria showing marked differences ($P < 0.2$) between targeted groups were selected from each cluster of phyla, genera, and OTUs (> 1% of the detected community).

Phylogenetic trees were constructed with MEGA7, MUSCLE, and iTOL (<https://itol.embl.de/>).

Stable isotope analysis of carbon and nitrogen

The isotopic compositions of carbon and nitrogen were determined by DELTA V Advantage (Thermo Fisher Scientific, USA) and Flash EA1112 (Thermo Fisher Scientific, USA), which were owned by Shoko Science Co., Ltd., Japan, according to the conventional protocol⁵²⁻⁵⁵ with some modifications. In brief, the total carbon and total nitrogen of the samples were measured by Flash EA1112 as follows: The oxidation and reduction reactors were heated to 1000 and 680°C, respectively. The carrier gas (He) flow was approximately 100 mL/min. The length of the separation column was 3 m. The oven temperature of the column was set at 35°C. Acetanilide (Kishida Chemical, Japan) was used as a standard. Stable carbon and nitrogen were measured by using elemental analyzer/isotope ratio mass spectrometry (EA/IRMS), a unit of Delta V Advantage interfaced with FlashEA 1112 as follows: The oxidation and reduction reactors were heated to 1000 and 680°C, respectively. The carrier gas (He) flow was approximately 100 mL/min. The length of the separation column was 3 m. The oven temperature of the column was set at 35°C. CO₂ gas and N₂ gas were used as the reference gases for the

detection of stable carbon and stable nitrogen, respectively. The working standards, Vienna Pee Dee Belemnite (VPDB) for carbon ($\delta^{13}\text{C}$), used alanine(19.6 ‰), histidine (10.7 ‰), and glycine (33.8 ‰). The working standards, air for nitrogen ($\delta^{15}\text{N}$), used alanine (1.58 ‰), alanine (9.97 ‰), and glycine (20.6 ‰). These standards were also prepared by Shoko Science Co., Ltd., Japan. The levels of chemical indices were visualized by using Prism software.

Association analyses

Association analysis⁵⁶⁻⁵⁸ is a technically established method in predictive science and is generally applied to understand the relations between one component and others by using relative values. It is convenient to apply when there are missing values as a characteristic of association analysis. Association rules were determined using criterion values of support, confidence, and lift as previously reported⁵⁶⁻⁵⁸. In brief, “support” is the probability of X and Y co-occurring in the transaction dataset:

$$\text{support } (X \Rightarrow Y) = P (X \cap Y)$$

The “confidence” of the rule $X \Rightarrow Y$ is the conditional probability of observing Y given that X is present in a transaction:

$$\text{confidence } (X \Rightarrow Y) = P (X \cap Y)/P (X)$$

The “lift” of the rule $X \Rightarrow Y$ is the ratio of the support if X and Y are independent:

$$\text{lift}(X \Rightarrow Y) = P(X \cap Y) / P(X) P(Y)$$

Therefore, higher lift values indicate a high probability of event Y in the case of condition X. Because lift values < 1 do not correlate (independent relationship) between X and Y as association rules, this study adopted a cutoff value of 1.3 as a lift value threshold for association rules. X and Y are represented here as the “source” and “target”, respectively. The analysis, also called a market basket analysis, was performed with the packages “arules” and “aruleViz” in R software (version 4.0.5) (<https://cran.r-project.org>). The association analysis parameters were set as “support = 0.063, confidence = 0.25, maxlen = 2” and “lift > 1.3”. The systemic network was rendered by Force Atlas, Fruchterman Reingold, and Noverlap in Gephi 0.9.2 (<http://gephi.org>). Sankey diagrams⁵⁹ for carbon and nitrogen flow were visualized by the packages “networkD3”, “tibble”, and “tidygraph” in R software. For the bacteria as a source, those directly involved in targeting $\delta^{13}\text{C}$, $\delta^{15}\text{N}$ carbon, and nitrogen were selected from Figs. 5 and 6. The values of the diagrams were calculated based on the difference in levels of $\delta^{13}\text{C}$, $\delta^{15}\text{N}$ carbon, and nitrogen between the habitat (M-chips) and the feces (Feces) (Fig. 3) in each box (Table S1). The classification of increase ($_H$) and/or decrease ($_L$) in the diagrams was also determined in the same way.

Structural Equation Modeling

Structural equation modeling (SEM) for confirmatory factor analysis (CFA) was conducted using the package “lavaan”^{60,61} of R software. The analysis codes were referred to the website (<https://lavaan.ugent.be>). Since CFA needs a hypothesis, the bacterial groups selected by association analysis were utilized as factors for a latent construct of metabolism of carbon, nitrogen, and their isotopes. The models as hypotheses were statistically estimated using maximum likelihood (ML) parameter estimation with bootstrapping (n = 1000) by the functions ‘lavaan’ and ‘sem’. Model fit was assessed by the chi-squared p-value ($p > 0.05$, nonsignificant), comparative fit index (CFI) (> 0.9), root mean square error of approximation (RSMEA) (< 0.05), and standardized root mean residuals (SRMR) (< 0.08) as indices of good model fit⁶². The path diagrams of the good model were visualized using the package “semPlot” of R software⁶³.

Other statistical analyses for verification of SEM

Individual causal mediation analyses were evaluated using the package “mediation” of R software⁶⁴. The analysis codes were referred to the tutorial website (<https://rpubs.com/Momen/485122>). Each regression relationship with ‘~’ in the selected

model was assessed by using the function ‘lm’, and thereafter, the values of the causal relationship between bacterial candidates as mediators and outcomes were evaluated using the function ‘mediation’, and the estimated average causal mediation effect (ACME), average direct effect (ADE), and proportion of total effect via mediation were calculated by quasi-Bayesian approximation (‘boot=FALSE’ as a command) and nonparametric bootstrapping (‘boot=TRUE’) with ‘sims=1000’.

Furthermore, to estimate a structural model beyond the distribution of limited experimental data, linear non-Gaussian acyclic models (LiNGAM)⁶⁵, which is an independent component analysis and a non-Gaussian method for estimating causal structures, and BayesLiNGAM⁶⁶, which is a Bayesian score-based approach to take advantage of non-Gaussianity when estimating linear acyclic causal models, were applied for the selected bacterial groups related to the metabolism of carbon and nitrogen.

LiNGAM was established with Python code on the website (<https://github.com/cdt15/lingam>) (Python version 3.6). The analysis procedure was also

based on other website information

(<https://qiita.com/DS27/items/4fe51cfc8c8183b1babf>). The data calculated by LiNGAM were visualized as networks by Gephi. BayesLiNGAM was established by the packages “fastICA” of R software based on the specialized prepared website information

(<https://www.cs.helsinki.fi/group/neuroinf/lingam/bayeslingam/>). The analysis procedure was analyzed by the packages “fastICA” of R software referred to the other website information (<https://qiita.com/kumalpha/items/038e85155374d49d8aa1>). The data calculated by BayesLiNGAM were visualized as networks by the R package “igraph”.

Statistical analysis

The procedure for statistical analysis was described above for each method. Significance was declared at $P < 0.05$, and a tendency was assumed at $0.05 \leq P < 0.20$. The data are presented as the means \pm SE.

Result

Microbial analysis

The fecal bacterial flora of Japanese rhinoceros beetle (*T. dichotomus*) larvae and the wood chips used as their habitat beds were examined. After subculturing the beetles alone and mating them within the same box for two years, the relationship between the bacterial community of the larvae and their habitat was analyzed after replacement of wood chips and maintenance under stable conditions for one month before the larvae became pupae

(Table S1). Despite the presence of different environmental microorganisms (Group I and Group II), the predominant bacterial community and bacterial diversities did not appear to change significantly (Fig. 2a and Fig. S1), but the phyla Chloroflexi^{67,68}, Gemmatimonadetes⁶⁹, and Planctomycetes⁷⁰ did change as the minor bacterial composition increased (Figs. 2, S2a). Next, the relative abundances of bacteria present under both conditions were examined for approximately 30% of the bacterial genera in the major community (comparison of bacteria with an abundance >1% of the total bacterial abundance) (Fig. S2b). The markedly enriched bacteria in the feces were as follows (enriched fecal bacteria) (Fig. 2bc): the genus *Corallococcus*, members of which have anti-gram-negative activity and act as natural antibiotics⁷¹; the genus *Gemmata*, which is involved in anaerobic ammonium oxidization (anammox)⁶⁹ and is classified in Gemmatimonadetes; the genera *Chonella*, *Hyphomicrobium*, and *Paenibacillus*, which are nitrogen-fixing bacteria (rhizobia)⁷²⁻⁷⁴; the genus *Lutibacterium*, which includes a bacterium that can degrade hydrocarbons and is a candidate for use in bioremediation⁷⁵; *Rhodoplanes*, a genus of bacteria that produce hopanoids⁷³; and the genus *Bradyrhizobium*, which is a genus of nitrogen-fixing bacteria that affects plant growth and belongs to the phylum Proteobacteria, and bacteria with sequences belonging to the phylum Actinobacteria⁷⁶ (Figs. 2bc and S3). When compost was added externally, no

significant difference in the bacterial population in excreted feces appeared. The phylogenetic tree with relative abundances of 15 OTU-assigned bacteria with marked differences ($p < 0.2$) is shown (Fig. S4a). These bacteria were not always phylogenetically closely related to each other. OTU-4121, OTU-3393, and OTU-6, closely related to the genera *Corallocooccus*, *Lutibacterium*, and *Rhodoplanes*, were markedly enriched in the feces (Fig. S 4b). OTU-4009, which is closely related to the phylum Verrucomicrobia, was also enriched.

Correlation analysis of bacterial communities

When the correlations among these bacterial groups in wood chips and feces were investigated, the phyla Chloroflexi^{67,68}, Gemmatimonadetes⁶⁹, and Planctomysetes⁷⁰ were enriched in the feces and showed only slight correlations among themselves in the habitat (Fig. 3a). The genera *Corallocooccus*⁷¹, *Gemmata*⁶⁹, *Chonella*⁷², *Hyphomicrobium*^{77,78}, *Paenibacillus*⁷⁴, *Lutibacterium*⁷⁵, and *Rhodoplanes*^{73,79}, which were enriched in the feces, were not always correlated among themselves in the habitat (Fig. 3b). These relationships indicate that increases in bacterial abundance in the feces appear to be independent of the increases in bacterial abundance in the habitat. A positive correlation in the fecal community was shown between the phyla Planctomysetes⁷⁰ and

Verrucomicrobia, and a negative correlation was shown between the phyla Gemmatimonadetes and Firmicutes (Fig. S5a). The genus *Chonella* showed a positive correlation with the genera *Paenibacillus*, *Clostridium*, *Cellulomonas*, *Methanobacterium*, and *Pseudonocardia* within the feces (Fig. S5b). The genus *Paenibacillus* showed a negative correlation with the genera *Devosia* and *Rhodoplanes*. The genus *Gemmata* showed a negative correlation with the genus *Candidatus Xiphinematobacter*. The genus *Rhodoplanes* showed a positive correlation with the genera *Hyphomicrobium*, *Pedomicrobium*, *Planctomyces*, and *Devosia*. The genus *Hyphomicrobium* showed a positive correlation with the genera *Burkholderia*, *Sphingomonas*, and *Pilimelia*. The genus *Bradyrhizobium* showed a positive correlation with the genera *Fimbrimonas*, *Gemmatimonas*, *Pilimelia*, *Hyphomicrobium*, *Pedomicrobium*, *Planctomyces*, *Devosia*, and *Rhodoplanes* but a negative correlation with *Elin506*, *Bacillus*, and *Coprococcus*. The two genera *Lutibacterium* and *Corallocooccus* showed a negative correlation with the genus *Optitutus*. The genus *Corallocooccus* showed a positive correlation with the genera *Burkholderia*, *Sphingomonas*, *Hyphomicrobium*, *Pedomicrobium*, and *Planctomyces*. In addition, the patterns of these bacterial relationships in the habitat were different from those of the

fecal bacterial relationships (Fig. S6). The abundances of these bacteria in the feces were not necessarily positively correlated with the abundances of microorganisms in the habitat.

Carbon and nitrogen levels and their correlation with the bacterial community

The functional roles of the bacterial community were validated by evaluating the levels of chemical indices, *i.e.*, stable isotopes ($\delta^{13}\text{C}$ and $\delta^{15}\text{N}$), total carbon, total nitrogen, and the carbon/nitrogen (CN) ratio, in the wood chips and feces. Measurement of the stable isotope contents is known to be useful for inferring metabolic trends in dietary carbon and nitrogen of insects²³. The raw chips used as fresh chips for the habitat, decayed chips (M_chips), and feces, as shown in Fig. S7a, were examined. The levels in both decayed chips and feces were confirmed to be significantly different from those in fresh raw chips. In particular, the nitrogen level, $\delta^{15}\text{N}$ content, and total N content were clearly higher in the excreted feces of the beetle larvae (Figs. 4a and S7b). As a result, the CN ratio also appeared to decrease in the feces. This tendency was slightly changed in M-chips when compost was added externally, but no significant difference was confirmed in excreted feces. As seen in Fig. 4b, a correlation analysis including the chemical indices showed positive correlations between total nitrogen and *Lutibacterium*, *Paenibacillus*, and *Chonella*. In addition, the genera *Candidatus Solibacter* and *Sphingomonas* showed

negative correlations with total nitrogen. The $\delta^{15}\text{N}$ content showed a weak negative correlation with the genera *Sphingomonas* and *Clostridium*. The total carbon content showed negative correlations with the genera *Coralloccoccus*, *Lutibacterium*, *Paenibacillus*, and *Chonella* and a positive correlation with the genus *Candidatus Solibacter*. The $\delta^{13}\text{C}$ content showed a positive correlation with the genera *Lutibacterium* and *Elin506* and a negative correlation with the genera *Burkholderia*, *Devosia*, *Sphingomonas*, *Pilimelia*, and *Fimbrimonas*. The CN ratio showed negative correlations with the genera *Cellulomonas*, *Pseudonocardia*, and *Methanobacterium*.

Predictive selection of the bacterial community for carbon-nitrogen metabolism

Association analysis⁵⁶⁻⁵⁸, a technically established method in predictive science, was applied to evaluate the correlations of chemical indices and microbial communities in excreted feces beyond the bacterial taxonomic boundaries of the genus and phylum levels. The results showed that the systemic network of the indices and the bacteria in decayed chips and feces could be classified into four categories (Fig. S8). Based on the calculated lift values, the networks among the indices and the bacteria enriched in the feces are represented in Fig. S9. The associations of the bacterial genera *Coralloccoccus*, *Gemmata*, *Hyphomicrobium*, and *Lutibacterium* increased in the feces. The other enriched and

unenriched fecal bacteria were linked via feces-associated bacteria and/or other bacteria (Figs. S9 and S10). The chemical indices were strongly linked with not only the bacteria enriched in the feces but also bacteria that showed an inverse correlation with the indices. $\delta^{13}\text{C}$ was linked with the phylum Acidobacteria, which was linked with the genus *Elin506*, which in turn was linked with enriched fecal bacteria. A high level of $\delta^{13}\text{C}$ was modulated by a group in relation to increased phylum Acidobacteria, decreased phylum Armatimonadetes and genus *Sphingobium* (Fig. 5a). A low level of $\delta^{13}\text{C}$ was modulated by a group in relation to decreased phylum Acidobacteria and increased phylum Armatimonadetes, genera *Bradyrhizobium*, *Fimbrimonas*, *Methanobacterium*, and *Sphingobium* (Fig. 5a). $\delta^{15}\text{N}$ was linked with not only *Gemmata*, which was enriched in the feces but also the genera *Fimbrimonas* and *Methanobacterium*, which were not always enriched there. A high level of $\delta^{15}\text{N}$ was modulated by a group in relation to the increased phylum Armatimonadetes and genera *Gemmata*, *Fimbrimonas*, and *Methanobacterium* (Fig. 5b). A low level of $\delta^{15}\text{N}$ was modulated by a group in relation to the decreased phylum Armatimonadetes and genus *Gemmata* (Fig. 5c). The total carbon content was linked with not only *Bradyrhizobium*, one of the enriched fecal bacteria but also the phylum Bacteroidetes and genus *Candidatus Solibacter*, which were linked with some of the enriched fecal bacteria (Fig. S9). In particular, a high level of

total carbon content was assessed to be modulated by a group in relation to increased genera *Bradyrhizobium* and *Candidatus Solibacter* (Fig. 6a), and a low level of one was assessed to be modulated by a group in relation to decreased genera *Bradyrhizobium* and *Candidatus Solibacter* (Fig. 6b). The total nitrogen content was linked with the genus *Gemmatimonas*, which was linked with the genus *Pilimelia*, which in turn was linked with enriched fecal bacteria (Fig. S9). A high level of total nitrogen content was modulated by a group in relation to the increased genus *Gemmatimonas* and decreased genera *Devosia*, *Optitus*, and *Sphingobium* (Fig. 6b). A low level of total nitrogen content was modulated by a group in relation to the decreased genus *Gemmatimonas* and increased genera *Devosia*, *Optitus*, *Methanobacterium*, and *Sphingobium* (Fig. 6a). The CN ratio was linked with the enriched fecal bacteria via the genera *Devosia*, *Methanobacterium*, and *Sphingobium*, minor members of the fecal bacterial population. A high CN ratio content was modulated by a group in relation to the decreased genus *Gemmatimonas* and increased genera *Devosia*, *Methanobacterium*, *Optitus*, and *Sphingobium* (Fig. 6c). A low CN ratio was modulated by a group in relation to the increased genus *Gemmatimonas* and decreased genera *Devosia*, *Optitus*, and *Sphingobium* (Fig. 6d).

These observations indicated the possibility that the metabolism of carbon and nitrogen was associated with the enriched fecal bacteria as well as with other bacteria that were the minority of the fecal bacterial population and were inversely correlated with these indicators.

Structural equation modeling of the bacterial community for carbon-nitrogen metabolism

Since bacterial groups involved in carbon and nitrogen metabolism could be predicted by association analysis, structural equation models based on these hypotheses were created. As a result, we were able to construct relatively ideal structural models for the goodness-of-fit indices (Tables S2), which could be analyzed by bootstrapping using the maximum likelihood method even when the number of samples was relatively small. First, a bacterial group associated with stable isotope carbon $\delta^{13}\text{C}$ selected by the association analysis (Fig. 5a) was statistically tested as a hypothesized factor, and a regression group with Acidobacteria, Armatimonadetes, *Bradyrhizobium*, and *Sphingobium* was a suitable structural model with the highest goodness of fit for stable isotope carbon metabolism (Fig. 7a) compared to other models (Table S2). A suitable model for the metabolism of stable isotope nitrogen $\delta^{15}\text{N}$ was confirmed within the group shown in Fig. 5b by a similar

procedure, and a regression group with *Gemmata*, *Fimbrimonas*, *Methanobacterium*, *Armatimonadetes*, *Planctomycetes*, and *Gemmatimonadetes* was selected (Fig. 8b) compared to other models (Table S2). Suitable models for the metabolism of total carbon and nitrogen were selected (Figs. 8cd) compared to other models (Table S2). The suitable model of total carbon metabolism did not necessarily match the suitable model of metabolism of stable isotope carbon (Figs. 8ac), and *Bacteroidetes* was present in the structural model without *Bradyrhizobium* and *Candidatus Solibacter*. The suitable model of total nitrogen metabolism was inconsistent with the suitable model of metabolism of stable isotope nitrogen (Figs. 8bd). Within bacteria in the suitable model for metabolism of total nitrogen, *Bradyrhizobium*, *Sphingobium*, and/or *Candidatus Solibacter* were involved in models for metabolism of the stable isotope carbon and/or total carbon. *Paenibacillus*, *Optitus*, *Devosia*, and *Gemmatimonas* were characteristic within a model for total nitrogen metabolism. Stable bacteria that were not significantly different between M-chips and feces were selected as suitable models for carbon and nitrogen metabolism. Finally, the causal relationship in the bacterial group that had a regression relationship by SEM was statistically confirmed by causal mediation analysis (Tables S3-S6). As a result, it became clear that individual bacteria do not necessarily have a causal relationship except for some examples. In particular, the presence of the genus

Sphingobium and the phylum Armatimonadetes, minor bacteria, appeared to play an important role in the metabolism of stable isotope carbon $\delta^{13}\text{C}$ ($p=0.03799$ and $p=0.0235$, respectively). The presence of the genera *Fimbriimonas* and *Metanobacterium* and the phylum Armatimonadetes, minor bacteria, appeared to play an important role in the metabolism of stable isotope carbon $\delta^{15}\text{N}$, although not significant. The presence of the genus *Bradyrhizobium*, which was significantly increased in the feces, appeared to play an important role in the metabolism of total carbon ($p=0.0437$). The presence of genera *Corallocooccus* and *Paenibacillus*, which were significantly increased in the feces, appeared to play an important role in the metabolism of total nitrogen ($p=0.0442$ and $p=0.0557$, respectively). The presence of genera *Gemmatimonas*, *Opitutus*, *Candidus*, *Solibacter* and *Sphingobium*, minor bacteria, appeared to play an important role in the metabolism of total nitrogen, although not always significant.

Since the experimental data are limited in the actual data, it was necessary to be analyzed by using the maximum likelihood method based on the Gaussian distribution. However, it is not always clear whether original data in nature follow a Gaussian distribution. Therefore, assuming a non-Gaussian distribution, we analyzed the network with LiNGAM as an independent component analysis. Bacteria for the metabolism of $\delta^{13}\text{C}$, $\delta^{15}\text{N}$, total carbon, and total nitrogen in SEM with good fits were partly selected as causal

networks (Fig. S11). The selected causal networks may strongly show the causal relationship. The causal percentages of bacterial groups of SEM with good fits were also calculated by BayesLiNGAM. The predominant directed causal relationship was not always observed in bacterial groups for the metabolism of $\delta^{13}\text{C}$, $\delta^{15}\text{N}$, total carbon, and total nitrogen (Figs. S12). The percentages of the top 6 patterns of causal relationships were at low levels, although various patterns of directed causal relationships were calculated. These statistical observations may strongly suggest the importance of grouping the SEM-selected bacterial structure for the metabolism of carbon and nitrogen, not the effect by only a specific bacterium. Based on the observations, groups for carbon and nitrogen flows are visualized by Sankey diagrams (Fig.7).

These observations suggest that the bacteria involved in carbon and nitrogen metabolism should be affected not by specific predominant microorganisms but by the importance of the bacterial grouping structure as a group of multiple microorganisms. Regardless, structural equations with a high goodness of fit could be used to formulate a group using the results of association analysis as a hypothesis.

Discussion

The findings of this study suggested that potential environmentally beneficial bacteria may selectively grow in the intestines of beetle larvae and that the interactions between their predominant and other minor bacteria may regulate carbon and nitrogen flow from wood chips. Although the influence of other symbiotic microorganisms and hosts themselves except symbiotic bacteria may be considered on the metabolism of carbon and nitrogen, it became possible to infer the influence of the group by symbiotic bacteria, not the effect by only a specific bacterium. These bacterial candidates were detected by examining relative abundance, for example, the phylum Chroloflexi^{67,68}, members of which are known to have a nitrogen-oxidizing function⁸⁰. Bacteria belonging to the phyla Planctomycetes⁷⁰ and Gemmatimonadetes⁶⁹ potentiate the regulation of anaerobic ammonium oxidization (anammox)^{69,70}. *Gemmata*, an anammox bacterial genus⁶⁹, belongs to Gemmatimonadetes; the genera *Chonella*, *Hyphomicrobium*, and *Paenibacillus*, which are nitrogen-fixing and/or nitrogen-denitrifying bacteria (rhizobia)^{72-74,77,78}; and *Rhodoplanes*, a phototrophic genus that produces hopanoids^{73,79}, which are involved in the control of plant root growth and nitrogen fixation, are recognized as plant growth-promoting rhizobia (PGPRs). Among these findings, the presence of nitrogen-fixing bacteria in beetle larvae is consistent with previous data for other insects, such as termites (*Termitidae*)²⁰⁻²² and stag beetles (*Lucanidae*)³⁴, although the species of

nitrogen-fixing bacteria were different from those in previous studies. The presence of nitrogen-fixing, anammox, and hopanoid-producing bacterial candidates was shown in this insect. Furthermore, the genus *Lutibacterium*, which includes a bacterium that can degrade hydrocarbons and is a candidate for use in bioremediation ⁷⁵, and the genus *Corallococcus*, members of which have anti-gram-negative activity and act as natural antibiotics ⁷¹ were enriched under these conditions. Thus, the experiment conducted in this study showed enrichment of bacterial candidates with potential roles in plant-animal-environment symbiosis; these bacteria from beetle larval feces may be involved in nitrogen fixation, hopanoid production, anti-gram-negative interactions, anammox reactions and hydrocarbon degradation.

The symbiotic relationships of these bacteria and their functional roles were speculated by several evaluation methods. Although correlation analyses showed positive correlations between the total nitrogen content and *Lutibacterium*, *Paenibacillus*, and *Chonella* (Fig. 4c), association analyses predicted the association of chemical indices via the dilution of the minor fecal bacteria (Fig. 5b), which were inversely correlated with the enriched fecal bacteria (Fig. 4c). The total carbon content, CN ratio, $\delta^{15}\text{N}$ content, and $\delta^{13}\text{C}$ content also appeared to be associated with the other bacteria, which were minor members of the fecal bacterial community detected under the experimental conditions in

this study. These results suggest that the balance of the abundance ratio of dominant and inferior strains in the intestinal flora of beetle larvae may be involved in metabolism. The symbiotic phenomenon in which competition occurs among the intestinal bacterial community of insects is interesting, although the relevant study did not consider beetle larvae⁸¹. To the best of our knowledge, bacterial group candidates involved in the carbon and/or nitrogen cycle in the feces of beetle larvae were statistically estimated as an interactive network. SEM suggested that the metabolism of carbon, nitrogen, and their stable isotopes was composed of different groups. Causal mediation analysis revealed that the estimation is not significantly important as a single effect. These results were confirmed as trends regardless of parametric or nonparametric. LiNGAM was carried out on the assumption that it may not follow the Gaussian distribution in nature and visualized some causal relationships. These structural formulas did not fit perfectly, although they were partly fitted with the network constructed by SEM (Fig. S11). Such characteristics may become apparent under conditions with a non-Gaussian distribution depending on the environmental conditions. The causal percentages of bacterial groups of SEM were calculated by BayesLiNGAM, but the predominant directed causal relationship was not always observed (Figs. S12). This may suggest a spatial-temporal relationship of the bacterial population itself in the intestine. This study evaluated the relationship between

bacteria at the metabolic level under restricted experimental conditions and beetle larvae, but the modeling procedure in this study may be important. The bacterial behavior observed in this study may indirectly represent interactions with unknown factors, including other microorganisms. Future evaluations will be made on the relationship with other symbiotic microorganisms, such as fungi and the host itself. It is expected that the connection through the research will lead to a comprehensive understanding of the symbiotic system and will be useful for studying fermentation conditions using wood in an engineering manner.

Guessing the groups of microbial communities involved in carbon and nitrogen flow may be important in future studies. It may provide a new perspective on diversity in ecosystems and a hint for industrial utilization. In particular, the increasing trend in the $\delta^{15}\text{N}$ content in the feces may indicate that nitrogen from the wood chips was utilized for nutrition, as $\delta^{15}\text{N}$ is abundant in nitrogen obtained from plants⁸². Since the utilization of aerial nitrogen by stag beetle larvae was suggested³⁴, the nitrogen cycle of species other than beetles may be regulated through various steps. The nitrogen cycle-regulated bacterial group present in the larvae may be involved in protein synthesis. In relation to our observations, nitrogen cycle-regulated bacteria have been suggested to be abundant in the intestines of indigenous people who eat only plants and are muscular⁸³. A point of

view of the report is interesting, although it cannot be said unconditionally because the animal species are different.

Generally the growth stages of insects generally display physiological differences in relation to metabolism ²³. In addition, the microbial flora may change depending on symbiotic microorganisms and environments ^{11,84}. It has been pointed out that the microbial flora of beetles may change depending on the symbiotic microorganisms and the environment ^{9,10,12,85}. Therefore, it should be noted that our observations in this study were provided in a restricted environment just before the larvae became pupae. An important point of this study should be that it was possible to classify the groups of microorganisms involved in metabolic function, including potential association groups controlling carbon and nitrogen flow. Although these mechanisms were not clarified in this study, the certainty of the importance of these groups, which are involved in carbon and nitrogen flow, will be revealed in future studies. This is expected to be a point of view in assessing the role of insects in the ecosystem and in classifying the functionality of general intestinal flora, grouping from the function of complex microorganisms, which were grasped with the increase or decrease of complex microbial communities and metabolism.

Furthermore, from the perspective of ecosystem maintenance and industry, these observations remind us of the need for research from the following ones: The importance of the potential role of humic soil for beetles in the natural cycle, although rarely discussed to date, and the environmental roles in future industrial applications (Fig. 1b), *i.e.*, in circulating agriculture ⁸⁶, the prevention of plant and wood ^{87,88}, animal health ²⁵, and the prevention of global warming ⁸⁹. The finding that nitrogen-fixing and hopanoid-producing bacteria, which are useful for plants, were enriched in the feces of larvae fed wood is extremely important. The presence of these possibly useful bacteria in insect feces may be associated with the importance of humic soil, a compost used since ancient times. The enrichment of certain bacteria with natural antibiotics could be useful for the development of a novel feed additive to replace artificial antibiotics. In addition, the enrichment of certain bacteria with anammox and hydrocarbon degradation abilities could be useful for bioremediation and environmental protection. Thus, symbiotic bacteria from beetle larvae may be extremely important as candidate bacteria for agricultural recycling and environmental restoration and conservation, and reassessment of the functional grouping of candidate bacteria involved in carbon and nitrogen metabolism can be useful as a perspective on intestinal metabolism and environmental control. Attempts to understand the mechanism underlying the interactions and the roles

of environmentally symbiotic microbes of insects will be required to build a sustainable society.

Acknowledgments

We are grateful to Mrs. Miki Asakura, Mrs. Naoko Tachibana, Mrs. Sayo Suzuki, and Mrs. Naoko Atarashi (Riken IMS) for providing technical advice and support. We would like to express special thanks to Mrs. Izumi Jouzuka for helping with figure design.

Author contributions

Conceived and designed the experiments: H.M., K.I., and M.H.: performed subculturing and sampling: H.M. and K.I.: performed DNA extraction and the NGS experiment: F.A., W.S., M.M., C.S., and T.K.: analyzed the data: N.T., W.S., T.N., A.T., C.I., T.K., A.K., and H.S.: contributed reagents/materials/analysis tools: H.M., K.I., W.S., A.T., T.K., H.S., M.H., A.K., H.O., J.K., and H.K.: wrote the paper: H.M. and J.K.: revised the manuscript: H.M., H.S., S.M., M.H., M.H., H.O., J.K., and H.K.

Data availability

All 16S rRNA gene datasets were deposited in the DDBJ Sequence Read Archive (accession numbers: DRA012158). The R protocols for association analysis used in this study were deposited on the following website (<http://dmar.riken.jp/Rscripts/>)(<http://dmar.riken.jp/NMRinformatics/>).

Competing interests

The authors declare no competing interests.

References

- 1 Sánchez-Bayo, F. & Wyckhuys, K. A. G. Worldwide decline of the entomofauna: A review of its drivers. *Biological Conservation* **232**, 8-27, doi:10.1016/j.biocon.2019.01.020 (2019).
- 2 Lister, B. C. & Garcia, A. Climate-driven declines in arthropod abundance restructure a rainforest food web. *Proc Natl Acad Sci U S A* **115**, E10397-E10406, doi:10.1073/pnas.1722477115 (2018).
- 3 Welti, E. A. R. *et al.* Studies of insect temporal trends must account for the complex sampling histories inherent to many long-term monitoring efforts. *Nature Ecology and Evolution* **5**, 581-591, doi:<https://doi.org/10.1038/s41559-020-1269-4> (2020). (2021).
- 4 Crossley, M. S. *et al.* No net insect abundance and diversity declines across US Long Term Ecological Research sites. *Nat Ecol Evol* **4**, 1368-1376, doi:10.1038/s41559-020-1269-4 (2020).
- 5 Shah, A. A., Dillon, M. E., Hotaling, S. & Woods, H. A. High elevation insect communities face shifting ecological and evolutionary landscapes. *Curr Opin Insect Sci* **41**, 1-6, doi:10.1016/j.cois.2020.04.002 (2020).
- 6 Delgado-Baquerizo, M., Eldridge, D. J., Hamonts, K. & Singh, B. K. Ant colonies promote the diversity of soil microbial communities. *The ISME Journal* **13**, 1114-1118, doi:10.1038/s41396-018-0335-2 (2019).
- 7 Ortega-Martinez, I. J. *et al.* Assembly mechanisms of dung beetles in temperate forests and grazing pastures. *Sci Rep* **10**, 391, doi:10.1038/s41598-019-57278-x (2020).
- 8 Ceballos, G., Ehrlich, P. R. & Dirzo, R. Biological annihilation via the ongoing sixth mass extinction signaled by vertebrate population losses and declines. *Proc Natl Acad Sci U S A* **114**, E6089-E6096, doi:10.1073/pnas.1704949114 (2017).
- 9 Kudo, R., Masuya, H., Endoh, R., Kikuchi, T. & Ikeda, H. Gut bacterial and fungal communities in ground-dwelling beetles are associated with host food habit and habitat. *ISME J* **13**, 676-685, doi:10.1038/s41396-018-0298-3 (2019).
- 10 Shukla, S. P., Sanders, J. G., Byrne, M. J. & Pierce, N. E. Gut microbiota of dung beetles correspond to dietary specializations of adults and larvae. *Mol Ecol* **25**, 6092-6106, doi:10.1111/mec.13901 (2016).
- 11 Chen, B. *et al.* Gut bacterial and fungal communities of the domesticated silkworm (*Bombyx mori*) and wild mulberry-feeding relatives. *ISME J* **12**, 2252-2262, doi:10.1038/s41396-018-0174-1 (2018).
- 12 Bauer, E., Kaltenpoth, M. & Salem, H. Minimal fermentative metabolism fuels extracellular symbiont in a leaf beetle. *ISME J* **14**, 866-870, doi:10.1038/s41396-019-0562-1 (2020).

- 13 Wang, Z., Xin, X., Shi, X. & Zhang, Y. A polystyrene-degrading *Acinetobacter* bacterium isolated from the larvae of *Tribolium castaneum*. *Sci Total Environ* **726**, 138564, doi:10.1016/j.scitotenv.2020.138564 (2020).
- 14 Yang, S. S. *et al.* Biodegradation of polypropylene by yellow mealworms (*Tenebrio molitor*) and superworms (*Zophobas atratus*) via gut-microbe-dependent depolymerization. *Sci Total Environ* **756**, 144087, doi:10.1016/j.scitotenv.2020.144087 (2021).
- 15 Rockström, J. *et al.* A safe operating space for humanity. *Nature* **461**, 472-475 (2009).
- 16 Gao, L. & Bryan, B. A. Finding pathways to national-scale land-sector sustainability. *Nature* **544**, 217-222, doi:10.1038/nature21694 (2017).
- 17 Kang, J.-S., Shibuya, M. & Shin, C.-S. The effect of forest-thinning works on tree growth and forest environment. *Forest Science and Technology* **10**, 33-39, doi:10.1080/21580103.2013.821958 (2014).
- 18 Hsu, Y., Koizumi, H., Otagiri, M., Moriya, S. & Arioka, M. Trp residue at subsite - 5 plays a critical role in the substrate binding of two protistan GH26 beta-mannanases from a termite hindgut. *Appl Microbiol Biotechnol* **102**, 1737-1747, doi:10.1007/s00253-017-8726-2 (2018).
- 19 Nishimura, Y. *et al.* Division of functional roles for termite gut protists revealed by single-cell transcriptomes. *ISME J* **14**, 2449-2460, doi:10.1038/s41396-020-0698-z (2020).
- 20 Vesala, R., Arppe, L. & Rikkinen, J. Caste-specific nutritional differences define carbon and nitrogen fluxes within symbiotic food webs in African termite mounds. *Scientific Reports* **9**, doi:10.1038/s41598-019-53153-x (2019).
- 21 Desai, M. S. & Brune, A. Bacteroidales ectosymbionts of gut flagellates shape the nitrogen-fixing community in dry-wood termites. *ISME J* **6**, 1302-1313, doi:10.1038/ismej.2011.194 (2012).
- 22 Ohkuma, M. *et al.* Acetogenesis from H₂ plus CO₂ and nitrogen fixation by an endosymbiotic spirochete of a termite-gut cellulolytic protist. *Proc Natl Acad Sci U S A* **112**, 10224-10230, doi:10.1073/pnas.1423979112 (2015).
- 23 Chikayama, E., Suto, M., Nishihara, T., Shinozaki, K. & Kikuchi, J. Systematic NMR analysis of stable isotope labeled metabolite mixtures in plant and animal systems: coarse grained views of metabolic pathways. *PLoS One* **3**, e3805, doi:10.1371/journal.pone.0003805 (2008).
- 24 Alvarez, C., Reyes-Sosa, F. M. & Diez, B. Enzymatic hydrolysis of biomass from wood. *Microb Biotechnol* **9**, 149-156, doi:10.1111/1751-7915.12346 (2016).

- 25 DiGiacomo, K. & Leury, B. J. Review: Insect meal: a future source of protein feed for pigs? *Animal* **13**, 3022-3030, doi:10.1017/S1751731119001873 (2019).
- 26 van Huis, A. Insects as food and feed, a new emerging agricultural sector: a review. *Journal of Insects as Food and Feed* **6**, 27-44, doi:10.3920/jiff2019.0017 (2020).
- 27 Jia, D. *et al.* Insect symbiotic bacteria harbour viral pathogens for transovarial transmission. *Nat Microbiol* **2**, 17025, doi:10.1038/nmicrobiol.2017.25 (2017).
- 28 Zhou, F. *et al.* Altered Carbohydrates Allocation by Associated Bacteria-fungi Interactions in a Bark Beetle-microbe Symbiosis. *Sci Rep* **6**, 20135, doi:10.1038/srep20135 (2016).
- 29 Koneru, S. L., Salinas, H., Flores, G. E. & Hong, R. L. The bacterial community of entomophilic nematodes and host beetles. *Mol Ecol* **25**, 2312-2324, doi:10.1111/mec.13614 (2016).
- 30 Akami, M. *et al.* Gut bacteria of the cowpea beetle mediate its resistance to dichlorvos and susceptibility to *Lippia adoensis* essential oil. *Sci Rep* **9**, 6435, doi:10.1038/s41598-019-42843-1 (2019).
- 31 Harrison, M. C. *et al.* Hemimetabolous genomes reveal molecular basis of termite eusociality. *Nat Ecol Evol* **2**, 557-566, doi:10.1038/s41559-017-0459-1 (2018).
- 32 Smith, S. M., Kent, D. S., Boomsma, J. J. & Stow, A. J. Monogamous sperm storage and permanent worker sterility in a long-lived ambrosia beetle. *Nat Ecol Evol* **2**, 1009-1018, doi:10.1038/s41559-018-0533-3 (2018).
- 33 Wang, Y. & Rozen, D. E. Gut Microbiota Colonization and Transmission in the Burying Beetle *Nicrophorus vespilloides* throughout Development. *Appl Environ Microbiol* **83**, doi:10.1128/AEM.03250-16 (2017).
- 34 Tanahashi, M., Ikeda, H. & Kubota, K. Elementary budget of stag beetle larvae associated with selective utilization of nitrogen in decaying wood. *The Science of Nature* **105**, 33, doi: 10.1007/s00114-018-1557-x (2018).
- 35 Hitch, T. C. A. *et al.* Automated analysis of genomic sequences facilitates high-throughput and comprehensive description of bacteria. *ISME Communications* **1**, doi:10.1038/s43705-021-00017-z (2021).
- 36 Schapheer, C., Pellens, R. & Scherson, R. Arthropod-Microbiota Integration: Its Importance for Ecosystem Conservation. *Front Microbiol* **12**, 702763, doi:10.3389/fmicb.2021.702763 (2021).
- 37 Ulyshen, M. D., Wagner, T. L. & Muller-Landau, H. Quantifying arthropod contributions to wood decay. *Methods in Ecology and Evolution* **4**, 345-352, doi:10.1111/2041-210x.12012 (2013).

- 38 Jang, S. & Kikuchi, Y. Impact of the insect gut microbiota on ecology, evolution, and industry. *Curr Opin Insect Sci* **41**, 33-39, doi:10.1016/j.cois.2020.06.004 (2020).
- 39 Bar-Shmuel, N., Behar, A. & Segoli, M. What do we know about biological nitrogen fixation in insects? Evidence and implications for the insect and the ecosystem. *Insect Sci* **27**, 392-403, doi:10.1111/1744-7917.12697 (2020).
- 40 Miyamoto, H. *et al.* Potential probiotic thermophiles isolated from mice after compost ingestion. *J Appl Microbiol* **114**, 1147-1157, doi:10.1111/jam.12131 (2013).
- 41 Tashiro, Y. *et al.* A novel production process for optically pure L-lactic acid from kitchen refuse using a bacterial consortium at high temperatures. *Bioresour Technol* **146**, 672-681, doi:10.1016/j.biortech.2013.07.102 (2013).
- 42 Ishikawa, K. *et al.* Denitrification in soil amended with thermophile-fermented compost suppresses nitrate accumulation in plants. *Appl Microbiol Biotechnol* **97**, 1349-1359, doi:10.1007/s00253-012-4004-5 (2013).
- 43 Niisawa, C. *et al.* Microbial analysis of a composted product of marine animal resources and isolation of bacteria antagonistic to a plant pathogen from the compost. *Journal of General and Applied Microbiology* **54**, 149-158 (2008).
- 44 Miyamoto, H. *et al.* Thermophile-fermented compost as a possible scavenging feed additive to prevent peroxidation. *J Biosci Bioeng* **116**, 203-208, doi:10.1016/j.jbiosc.2013.01.024 (2013).
- 45 Miyamoto, H. *et al.* The oral administration of thermophile-fermented compost extract and its influence on stillbirths and growth rate of pre-weaning piglets. *Res Vet Sci* **93**, 137-142, doi:10.1016/j.rvsc.2011.06.018 (2012).
- 46 Fu, G. *et al.* Effects of substrate type on denitrification efficiency and microbial community structure in constructed wetlands. *Bioresour Technol* **307**, 123222, doi:10.1016/j.biortech.2020.123222 (2020).
- 47 Wang, S. *et al.* Selectively enrichment of antibiotics and ARGs by microplastics in river, estuary and marine waters. *Sci Total Environ* **708**, 134594, doi:10.1016/j.scitotenv.2019.134594 (2020).
- 48 Caporaso, J. G. *et al.* QIIME allows analysis of high-throughput community sequencing data. *Nature Methods* **7**, 335-336, doi:org/10.1038/nmeth.f.303 (2010).
- 49 Kim, S. W. *et al.* Robustness of gut microbiota of healthy adults in response to probiotic intervention revealed by high-throughput pyrosequencing. *DNA Res* **20**, 241-253, doi:10.1093/dnares/dst006 (2013).
- 50 Said, H. S. *et al.* Dysbiosis of salivary microbiota in inflammatory bowel disease and its association with oral immunological biomarkers. *DNA Res* **21**, 15-25, doi:10.1093/dnares/dst037 (2014).

- 51 Jinnohara, T. *et al.* IL-22BP dictates characteristics of Peyer's patch follicle-associated epithelium for antigen uptake. *J Exp Med* **214**, 1607-1618, doi:10.1084/jem.20160770 (2017).
- 52 Satoh, R. & Suzuki, Y. Carbon and Nitrogen stable analysis by EA IRMS. *Res Org Geochem* **26**, 21-29 (2010).
- 53 Simsek, A., Bilsel, M. & Goren, A. C. 13C/12C pattern of honey from Turkey and determination of adulteration in commercially available honey samples using EA-IRMS. *Food Chemistry* **130**, 1115-1121, doi:10.1016/j.foodchem.2011.08.017 (2012).
- 54 Nakashita, R. *et al.* Stable carbon, nitrogen, and oxygen isotope analysis as a potential tool for verifying geographical origin of beef. *Anal Chim Acta* **617**, 148-152, doi:10.1016/j.aca.2008.03.048 (2008).
- 55 He, F. *et al.* Authentication of Processed Epimedii folium by EA-IRMS. *J Anal Methods Chem* **2020**, 8920380, doi:10.1155/2020/8920380 (2020).
- 56 Shiokawa, Y., Misawa, T., Date, Y. & Kikuchi, J. Application of Market Basket Analysis for the Visualization of Transaction Data Based on Human Lifestyle and Spectroscopic Measurements. *Analytical Chemistry* **88**, 2714-2719, doi:10.1021/acs.analchem.5b04182 (2016).
- 57 Shiokawa, Y., Date, Y. & Kikuchi, J. Application of kernel principal component analysis and computational machine learning to exploration of metabolites strongly associated with diet. *Sci Rep* **8**, 3426, doi:10.1038/s41598-018-20121-w (2018).
- 58 Wei, F., Sakata, K., Asakura, T., Date, Y. & Kikuchi, J. Systemic Homeostasis in Metabolome, Ionome, and Microbiome of Wild Yellowfin Goby in Estuarine Ecosystem. *Sci Rep* **8**, 3478, doi:10.1038/s41598-018-20120-x (2018).
- 59 Schmidt, M. The Sankey Diagram in Energy and Material Flow Management. *Journal of Industrial Ecology* **12**, 173-185, doi:10.1111/j.1530-9290.2008.00015.x (2008).
- 60 Rosseel, Y. lavaan: An R Package for Structural Equation. *Journal of Statistical Software* **48**, 1-36 (2012).
- 61 Rosseel, Y. *et al.* Latent Variable Analysis. *R package version 0.6-9* (2021).
- 62 Hooper, D., Coughlan, J. & Mullen, M. R. Structural equation modelling: guidelines for determining model fit. *Electron J Business Res Methods* **6**, 53-60 (2008).
- 63 Epskamp, S., Stuber, S., Nak, J., Veenman, M. & Jorgensen, T. D. Path Diagrams and Visual Analysis of Various SEM Packages' Output *R package version 1.1.2* (2019).
- 64 Tingley, D., Yamamoto, T., Hirose, K., Keele, L. & Imai, K. mediation: R Package for Causal Mediation Analysis. *Journal of Statistical Software* **59**, 1-38 (2014).
- 65 Shimizu, S., Hoyer, P. O., Hirshenko, A. H. & Kerminen, A. A Linear Non-Gaussian Acyclic Model for Causal Discovery. *Journal of Machine Learning Research*, 2003-2030 (2006).

- 66 Hoyer, P. O. & Hyttinen, A. Bayesian Discovery of Linear Acyclic Causal Models. *arXiv.org*, arXiv:1205.2641, doi:<https://arxiv.org/abs/1205.2641> (2009).
- 67 Igiehon, N. O., Babalola, O. O., Cheseto, X. & Torto, B. Effects of rhizobia and arbuscular mycorrhizal fungi on yield, size distribution and fatty acid of soybean seeds grown under drought stress. *Microbiol Res* **242**, 126640, doi:10.1016/j.micres.2020.126640 (2021).
- 68 Xu, T. *et al.* Characterization of the microbial communities in wheat tissues and rhizosphere soil caused by dwarf bunt of wheat. *Sci Rep* **11**, 5773, doi:10.1038/s41598-021-85281-8 (2021).
- 69 Xu, P. *et al.* High performance of integrated vertical-flow constructed wetland for polishing low C/N ratio river based on a pilot-scale study in Hangzhou, China. *Environ Sci Pollut Res Int* **26**, 22431-22449, doi:10.1007/s11356-019-05508-0 (2019).
- 70 van Teeseling, M. C. F. *et al.* Anammox Planctomycetes have a peptidoglycan cell wall. *Nature Communications* **6**, doi:10.1038/ncomms7878 (2015).
- 71 Livingstone, P. G. *et al.* Predatory Organisms with Untapped Biosynthetic Potential: Descriptions of Novel Coralloccoccus Species *C. aberystwythensis* sp. nov., *C. carmarthensis* sp. nov., *C. exercitus* sp. nov., *C. interemptor* sp. nov., *C. llansteffanensis* sp. nov., *C. praedator* sp. nov., *C. sicarius* sp. nov., and *C. terminator* sp. nov. *Appl Environ Microbiol* **86**, e01931-01919 (2020).
- 72 Li-Ying, W., Tian-Shu, W. & San-Feng, C. *Cohnella capsici* sp. nov., a novel nitrogen-fixing species isolated from *Capsicum annuum* rhizosphere soil, and emended description of *Cohnella plantaginis*. *Antonie Van Leeuwenhoek* **107**, 133-139 (2015).
- 73 Belin, B. J., Tookmanian, E. M., de Anda, J., Wong, G. C. L. & Newman, D. K. Extended Hopanoid Loss Reduces Bacterial Motility and Surface Attachment and Leads to Heterogeneity in Root Nodule Growth Kinetics in a Bradyrhizobium-Aeschynomene Symbiosis. *Molecular Plant-Microbe Interactions* **32**, 1415-1428, doi:10.1094/mpmi-04-19-0111-r (2019).
- 74 Grady, E. N., MacDonald, J., Liu, L., Richman, A. & Yuan, Z.-C. Current knowledge and perspectives of *Paenibacillus*: a review. *Microbial Cell Factories* **15**, doi:10.1186/s12934-016-0603-7 (2016).
- 75 Yakimov, M. M., Timmis, K. N. & Golyshin, P. N. Obligate oil-degrading marine bacteria. *Curr Opin Biotechnol* **18**, 257-266, doi:10.1016/j.copbio.2007.04.006 (2007).
- 76 Santamaría, R. I. *et al.* Characterization of Actinomycetes Strains Isolated from the Intestinal Tract and Feces of the Larvae of the Longhorn Beetle *Cerambyx welensii*. *Microorganisms* **8**, doi:10.3390/microorganisms8122013 (2020).

- 77 Martineau, C., Mauffrey, F. & Villemur, R. Comparative Analysis of Denitrifying Activities of *Hyphomicrobium nitrivorans*, *Hyphomicrobium denitrificans*, and *Hyphomicrobium zavarzinii*. *Appl Environ Microbiol* **81**, 5003-5014, doi:10.1128/AEM.00848-15 (2015).
- 78 Fesefeldt, A., Kloos, K., Bothe, H., Lemmer, H. & Gliesche, C. G. Distribution of denitrification and nitrogen fixation genes in *Hyphomicrobium* spp. and other budding bacteria. *Canadian Journal of Microbiology* **44**, 181-186, doi:10.1139/w97-139 (1998).
- 79 A, H. & Y, U. Rhodoplanes gen. nov., a New Genus of Phototrophic Bacteria Including *Rhodopseudomonas rosea* as *Rhodoplanes roseus* comb. nov. and *Rhodoplanes elegans* sp. nov. *International Journal of Systemic and Evolutionary Microbiology* **44**, 665-673, doi:<https://doi.org/10.1099/00207713-44-4-665> (1994).
- 80 Spieck, E. *et al.* Extremophilic nitrite-oxidizing Chloroflexi from Yellowstone hot springs. *The ISME Journal* **14**, 364-379, doi:10.1038/s41396-019-0530-9 (2019).
- 81 Itoh, H. *et al.* Host-symbiont specificity determined by microbe-microbe competition in an insect gut. *Proc Natl Acad Sci U S A* **116**, 22673-22682, doi:10.1073/pnas.1912397116 (2019).
- 82 Yoneyama, T. *et al.* Variation in Natural Abundance of ¹⁵N among Plant Parts and in ¹⁵N/¹⁴N Fractionation during N₂ Fixation in the Legume-Rhizobia Symbiotic System. *Plant and Cell Physiology* **27**, 791-799, doi:10.1093/oxfordjournals.pcp.a077165 (1986).
- 83 Igai, K. *et al.* Nitrogen fixation and nifH diversity in human gut microbiota. *Sci Rep* **6**, 31942, doi:10.1038/srep31942 (2016).
- 84 Fredensborg, B. L. *et al.* Parasites modulate the gut-microbiome in insects: A proof-of-concept study. *PLoS One* **15**, e0227561, doi:10.1371/journal.pone.0227561 (2020).
- 85 Wang, Y. & Rozen, D. E. Gut microbiota in the burying beetle, *Nicrophorus vespilloides*, provide colonization resistance against larval bacterial pathogens. *Ecol Evol* **8**, 1646-1654, doi:10.1002/ece3.3589 (2018).
- 86 Meng, F., Bar-Shmuel, N., Shavit, R., Behar, A. & Segoli, M. Gut bacteria of weevils developing on plant roots under extreme desert conditions. *BMC Microbiol* **19**, 311, doi:10.1186/s12866-019-1690-5 (2019).
- 87 Hartmann, M., Lee, S., Hallam, S. J. & Mohn, W. W. Bacterial, archaeal and eukaryal community structures throughout soil horizons of harvested and naturally disturbed forest stands. *Environ Microbiol* **11**, 3045-3062, doi:10.1111/j.1462-2920.2009.02008.x (2009).
- 88 Gossner, M. M., Beenken, L., Arend, K., Begerow, D. & Peršoh, D. Insect herbivory facilitates the establishment of an invasive plant pathogen. *ISME Communications* **1**, doi:10.1038/s43705-021-00004-4 (2021).

- 89 Hammer, T. J. *et al.* Treating cattle with antibiotics affects greenhouse gas emissions, and microbiota in dung and dung beetles. *Proc Biol Sci* **283**, doi:10.1098/rspb.2016.0150 (2016).

Figure legends

Fig. 1

- (a) This experiment investigated the bacterial population and total carbon and total nitrogen and their stable isotopes $\delta^{13}\text{C}$ and $\delta^{15}\text{N}$ in habitat chips of beetle larvae (bed for larvae) (M-chips) and their feces (Feces). Based on the observations, hypotheses for carbon and nitrogen metabolism in the feces of beetle larvae were established, and the hypotheses were statistically validated by structural equation modeling (SEM), causal mediation analysis (CMA), a linear non-Gaussian acyclic model (LiNGAM), and BayesLiNGAM.
- (b) Multiple putative roles as ecological cultivators of bacterial candidates for plant growth promotion, as feed additives, and for bioremediation among beetles, larvae, forests, agricultural fields, and industrial environments.

Fig. 2

- (a) Relative abundances of phyla in the microbiota in the habitat chips of beetle larvae (bed for larvae) (M-chips) and their feces (Feces)
- (b) Differences in phylum- and genus-level populations between the habitat (M-chips) and feces (Feces) ($n = 6$; $p < 0.2$; $> 1\%$ as the maximal value of the detected bacterial population among the whole population in each group). * indicates $p < 0.05$.
- (c) Estimation plots of representative phyla and (b) genera in Fig. 2a with their significance values ($p < 0.1$; $> 1\%$ as the maximal value of the detected bacterial population among the whole population in each group).

Fig. 3

Heatmaps of correlations between the habitat and fecal microbiota of beetle larvae:
(a) phyla and (b) genera.

Fig. 4

- (a) Estimation plots of stable isotope ($\delta^{13}\text{C}$ and $\delta^{15}\text{N}$) levels, carbon and nitrogen levels, and carbon/nitrogen ratios in the decayed chips (M-chips) and larval feces (Feces) represented in Fig. 6a
- (b) A heatmap of correlations between the components and the genera in beetle larvae feces is shown in Fig. 3a.

Fig. 5

Interactive systemic networks of factors associated with chemical indices and feces, which were shown with high ($_H$) or low ($_L$) levels based on the mediation values of the whole data of targeted components: (a), $\delta^{13}\text{C}$; (b) and (c), $\delta^{15}\text{N}$; (c) and (d), total carbon and nitrogen level. The bacteria and components in Fig. 1b

and Fig.3a are shown in bold letters. Bacteria with low populations (Fig.S9) are shown in violet.

Fig. 6

The relationship of fecal microbiota associated with (a) $\delta^{13}\text{C}$, (b) $\delta^{15}\text{N}$, (c) total carbon content, and (d) total nitrogen content was shown by structural equation modeling calculated for groups selected in Fig.5. Standardized β coefficients are reported. The abbreviation shows as follows: Brd, Bradyrhizobium ; Sph, Sphingobium; Acd, Acidobacteria ; Arm, Armatimonadetes ; Fmb, Fimbriimonas ; Gemmt, Gemmata ; Gmmtm, Gemmatimonadetes ; Pln, Planctomycetes; Mth, Methanobacterium ; Bct, Bacteroidetes ; C.S, Candidatus.Solibacter ; T_C, Total_C ; Crl, Corallococcus ; Dvs, Devosia ; Opt, Opitutus ; Pnb, Paenibacillus ; T_N, Total_N. Green positive; red, negative. The Fit indices were shown in Table S2.

Fig. 7

Carbon and nitrogen flows calculated by SEM in Fig.6 are visualized by Sankey diagrams: (a) $\delta^{13}\text{C}$, (b) $\delta^{15}\text{N}$, (c) total carbon content, and (d) total nitrogen content.

Supporting Information

Fig. S1

(a) OTU number and the Chao1, Shannon, and Simpson indices representing α -diversity in the habitat (M-chips) and feces (Feces). (b) UniFrac graph, unweighted and weighted, which shows β -diversities in the habitat (M-chips) and feces. (c) Values calculated based on unweighted and weighted data are shown under environmental conditions. I and II show environmental conditions: I, a group sprayed with water only; II, one sprayed with 20% compost extract.

Fig. S2

Relative abundances of (a) phyla and (b) genera in the habitat (M-chips) and feces (Feces) under environmental conditions. I and II show environmental conditions: I, a group sprayed with water only; II, one sprayed with 20% compost extract.

Fig. S3

(a) Estimation plots of representative phyla and (b) genera in Fig. 2b with their significance values ($0.1 < p < 0.2$; $> 1\%$ as maximal value of the detected bacterial population among the whole population in each group).

Fig. S4

(a) Phylogenetic tree and heatmap of representative bacterial OTUs in the feces ($p < 0.2$; $> 1\%$ as maximal value of the detected bacterial population among the whole population in each group).
(b) Estimation plots of representative OTUs in Fig. 3a with their significance values ($p < 0.1$; $> 1\%$ as maximal value of the detected bacterial population among the whole population in each group).

Fig. S5

Correlation heatmaps of the bacterial community in the feces of beetle larvae: (a) phyla and (b) genera.

Fig. S6

Correlation heatmaps of the bacterial community in the habitat of beetle larvae alone (a) phyla and (b) genera.

Fig. S7

Photographs of the samples used in this experiment (a) and stable isotope ($\delta^{13}\text{C}$ and $\delta^{15}\text{N}$) levels, carbon, and nitrogen levels and carbon/nitrogen ratios in the fresh wood chips of the habitat (raw chips), the decayed chips (M-chips), and larval feces (Feces). I and II show environmental conditions: I, a group sprayed with water only; II, one sprayed with 20% compost extract.

Fig. S8

Systemic networks of factors associated with chemical indices and feces. The factors shown in Figs. 2b and 6a are indicated with black lines. Modularity classes are discriminated by four colors, and lift values and the ratio are shown.

Fig. S9

Systemic networks of factors shown in Figs. 2b and 6a. The difference of color of nodes indicates strength of degree, whose value sums up the weights of the adjacent edges for each node. The bacteria and components in Figs. 2b and 6a are shown in bold letters. Stable bacteria, the population of which was not significantly different between the habitat and the feces (Fig. S10), are shown in violet.

Fig. S10

Estimation plots of stable bacterial genera of bacteria are shown in Fig. S9.

Fig. S11

Causal relationship estimated by LiNGAM. The LiNGAM values shows the extents of contribution.

Fig. S12

The top six groups composed by SEM estimated by BayesLiNGAM were visualized with percentages. The best appropriate groups calculated by SEM based on mediation values (M-chips and feces) in Fig. 7 were selected.

Table S1.

Body weights of larvae used in this experiment. One male larva and one female larva were bred in the same box for one month. I and II show environmental conditions: I, a group sprayed with water only; II, one sprayed with 20% compost extract

Table S2.

Statistical values of the final optimal structural equation models for $\delta^{13}\text{C}$, $\delta^{15}\text{N}$, total carbon, and total nitrogen in Fig. 6. Short terms in the table mean as follows: chisq, chi-square χ^2 ; df, degrees of freedom; p value, p-values (chi-square); cfi, comparative fit index; tli, Tucker–Lewis index; nfi, normed fit index; rfi, relative fit index; SRMR, standardized root mean residuals; AIC, Akaike information criterion; rmsea, root mean square error of approximation ; gfi, goodness-of-fit index; agfi, adjusted goodness-of-fit index. The No.1 column shows the best numerical structural equation model for $\delta^{13}\text{C}$, $\delta^{15}\text{N}$, total carbon, and total nitrogen, respectively. The No.2 column shows the inferior numerical structural equation models.

Table S3.

List of models targeted by causal mediation analysis (CMA) for $\delta^{13}\text{C}$ in Fig. 6 and their statistical values. Short terms in the table mean as follows: ACME, average causal mediation effects; ADE, the average direct effects.

Table S4.

List of models targeted by CMA for $\delta^{15}\text{N}$ in Fig. 6 and their statistical values. Short terms in the table mean as follows: ACME, average causal mediation effects; ADE, the average direct effects.

Table S5.

List of models targeted by CMA for total carbon in Fig. 6 and their statistical values. Short terms in the table mean as follows: ACME, average causal mediation effects; ADE, the average direct effects.

Table S6.

List of models targeted by CMA for total nitrogen in Fig. 6 and their statistical values. Short terms in the table mean as follows: ACME, average causal mediation effects; ADE, the average direct effects.

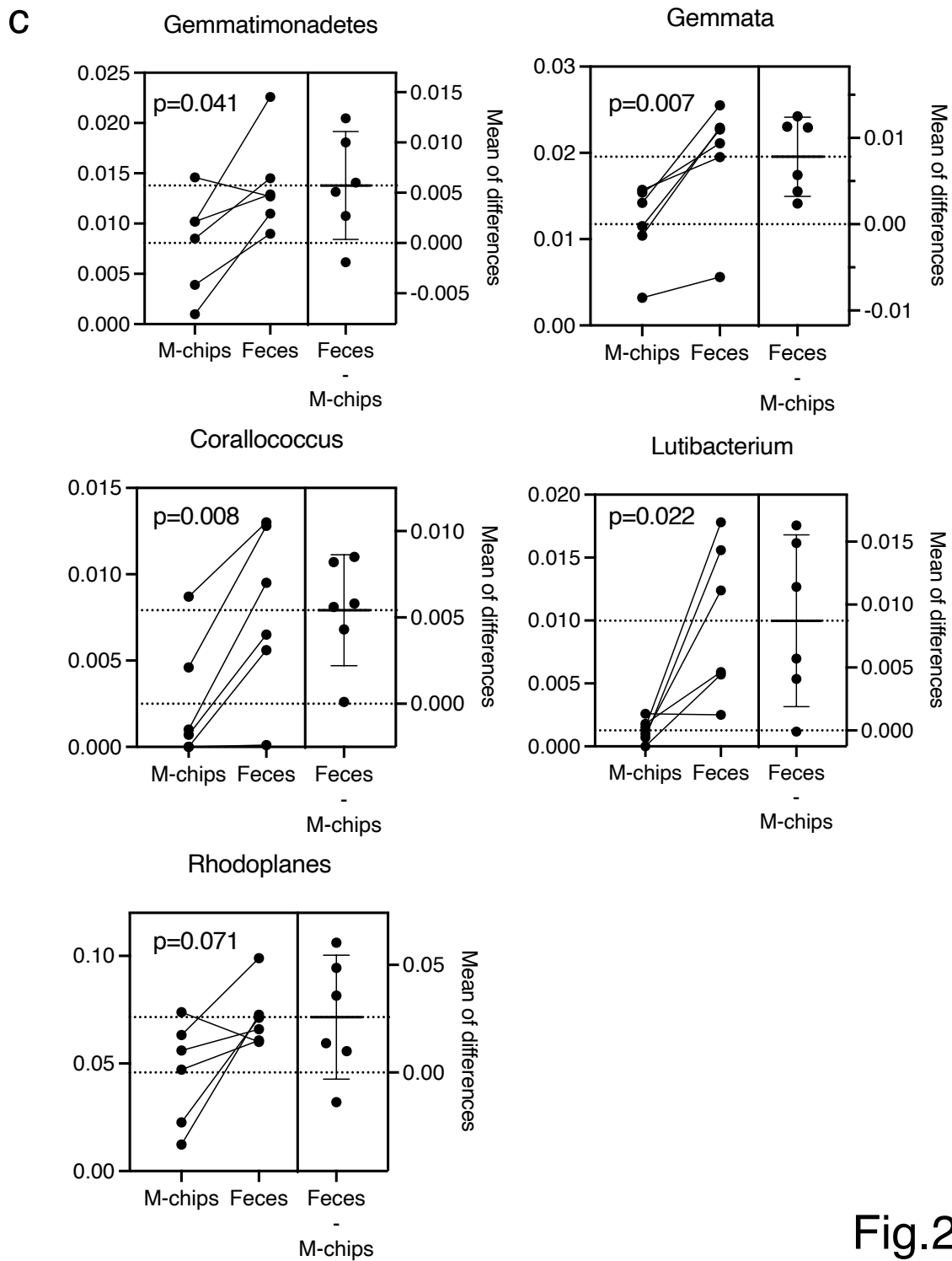
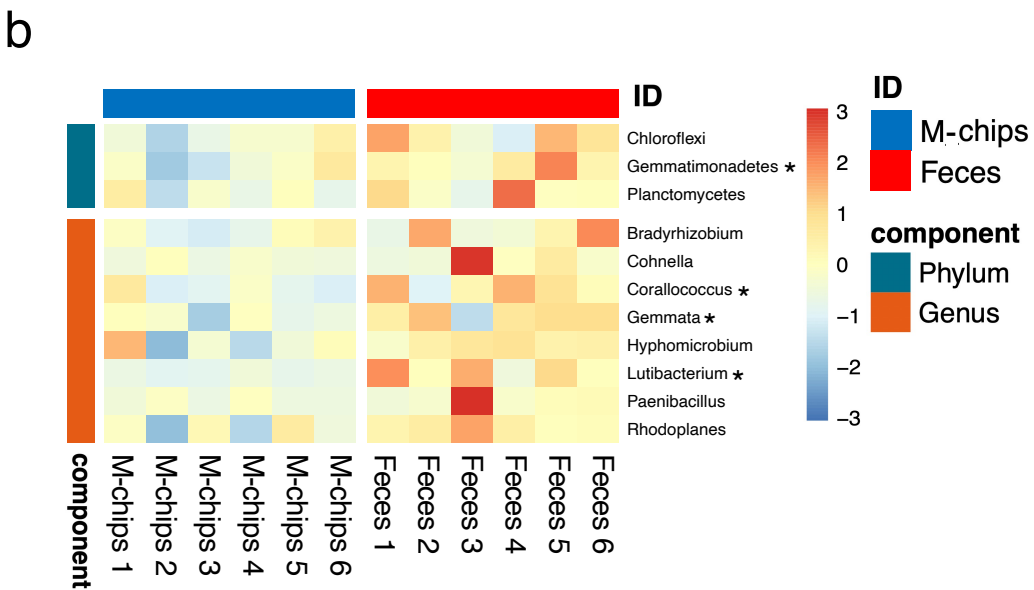
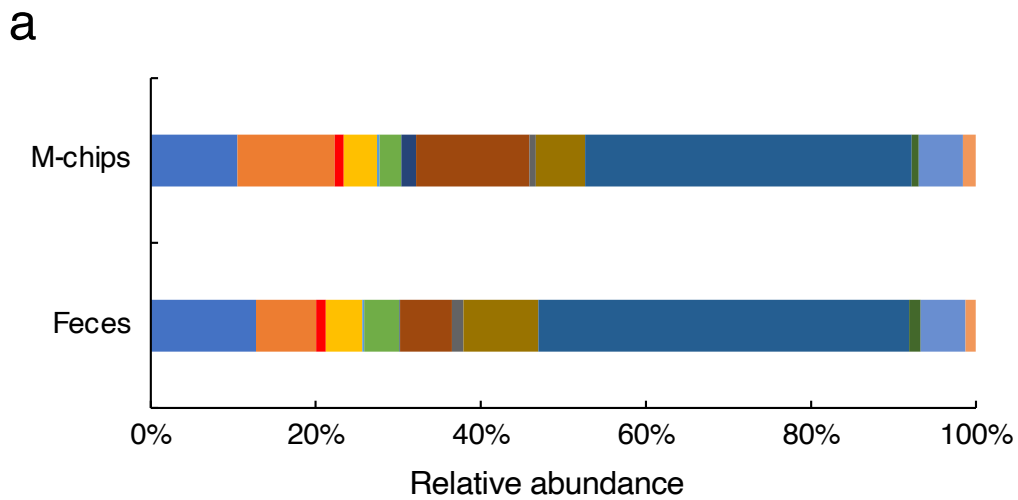
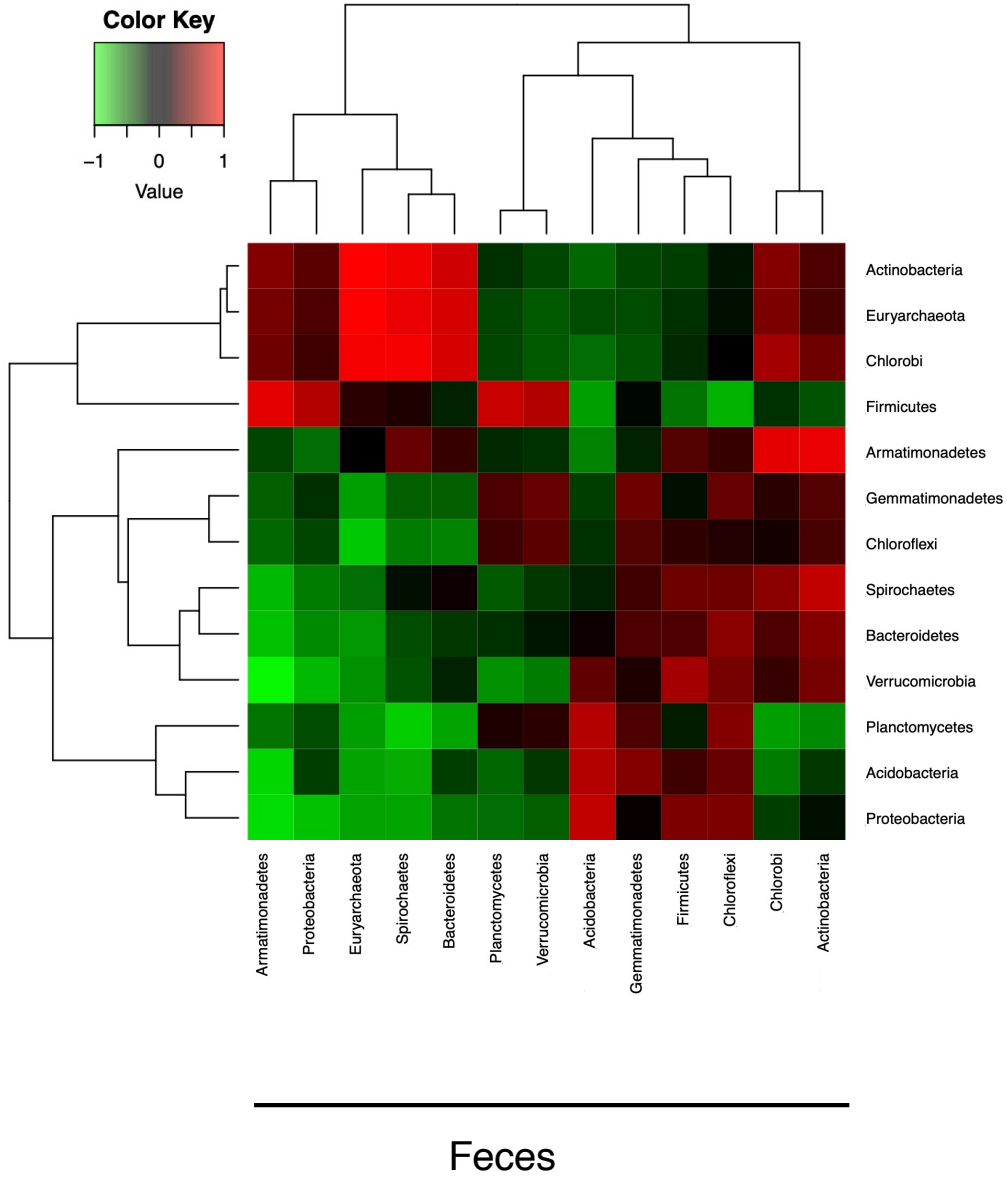


Fig.2

a



b

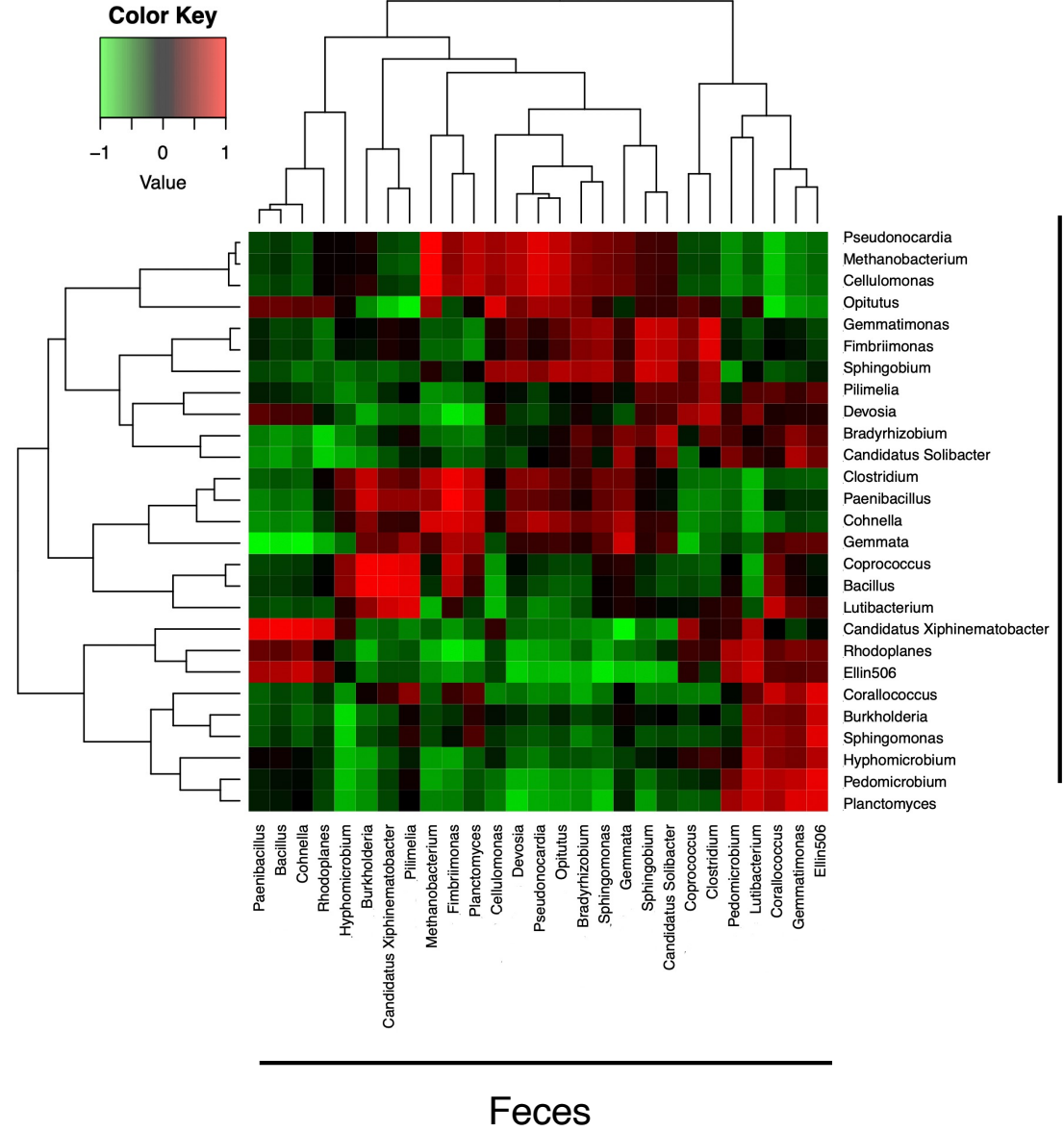


Fig.3

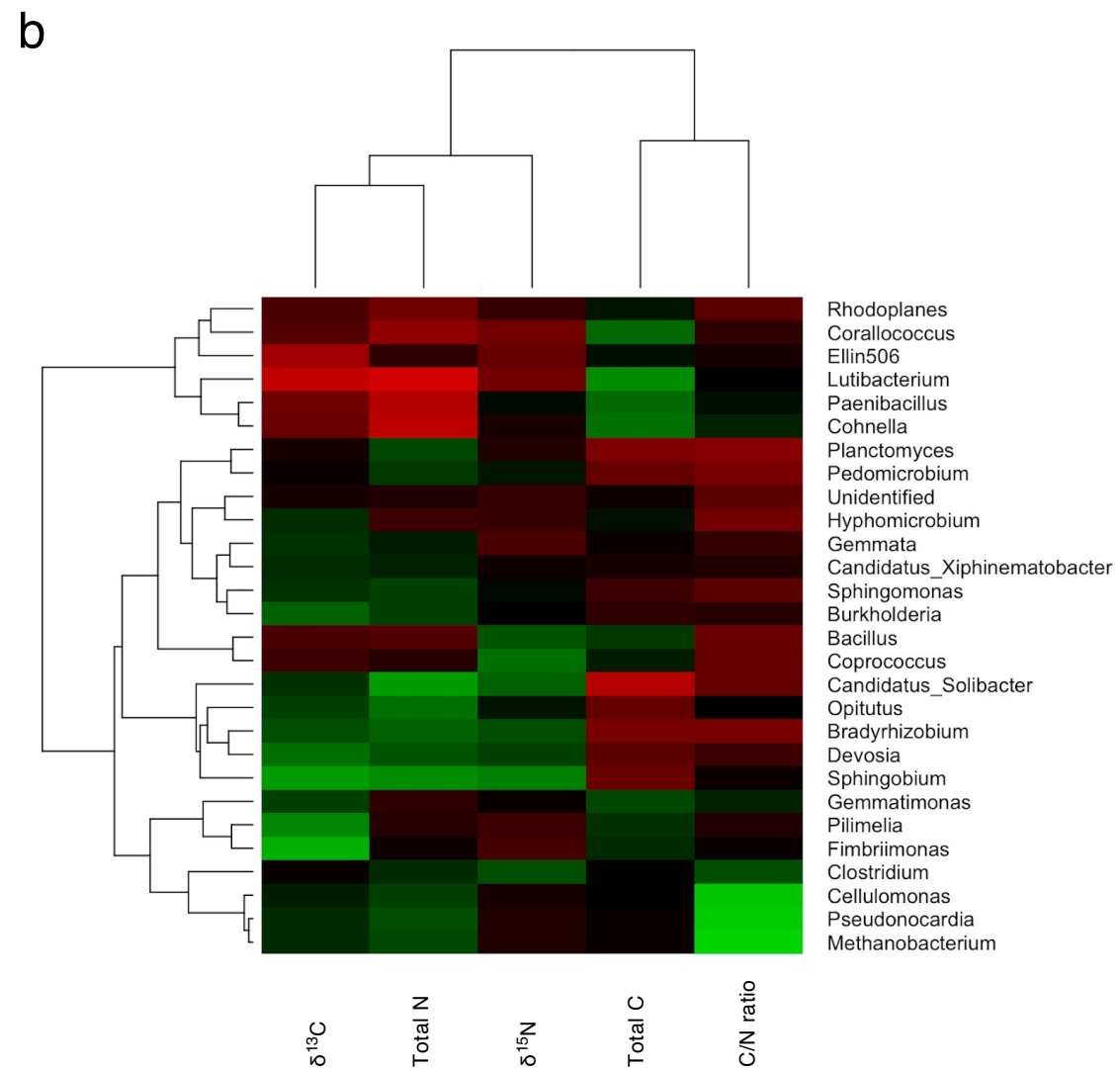
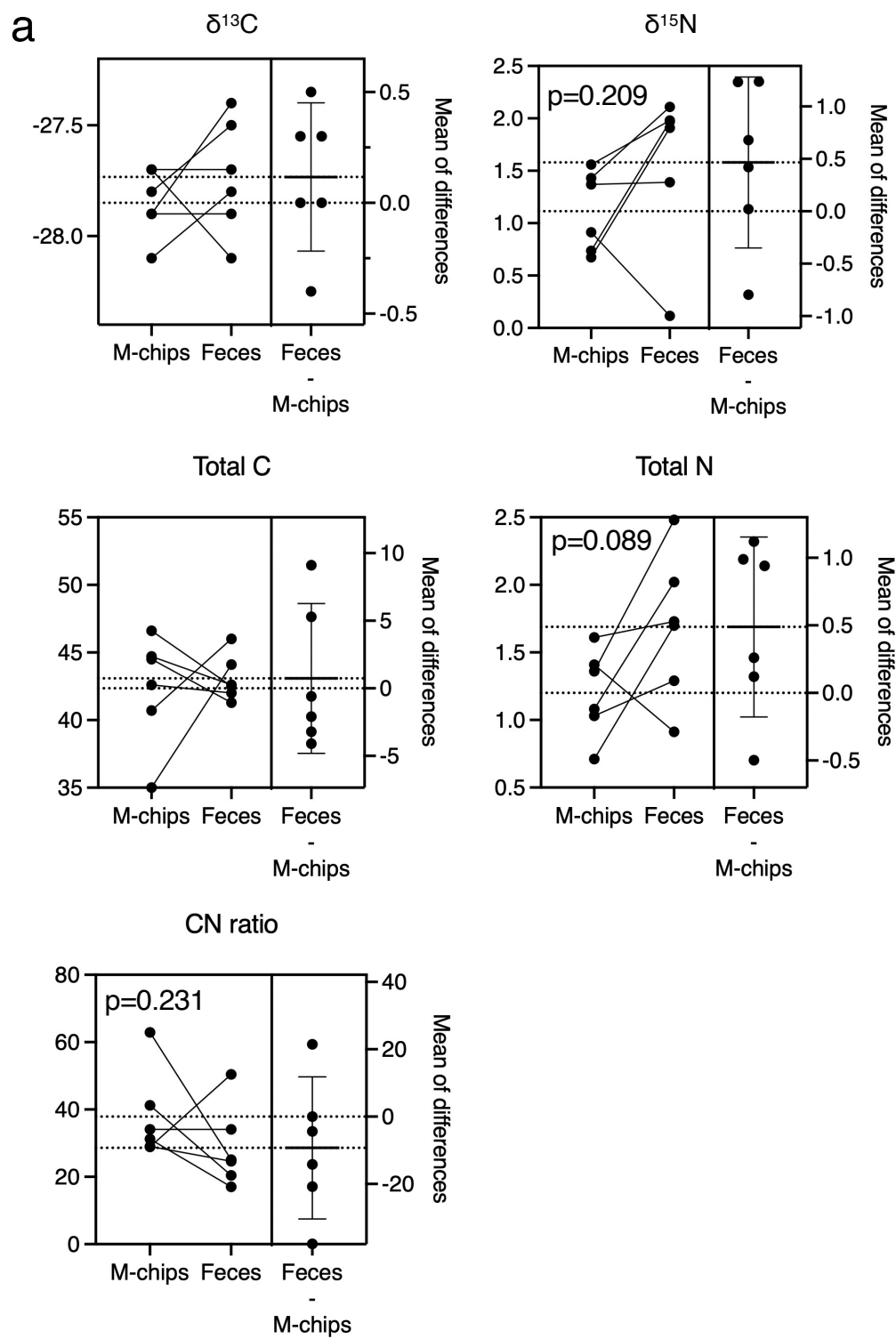
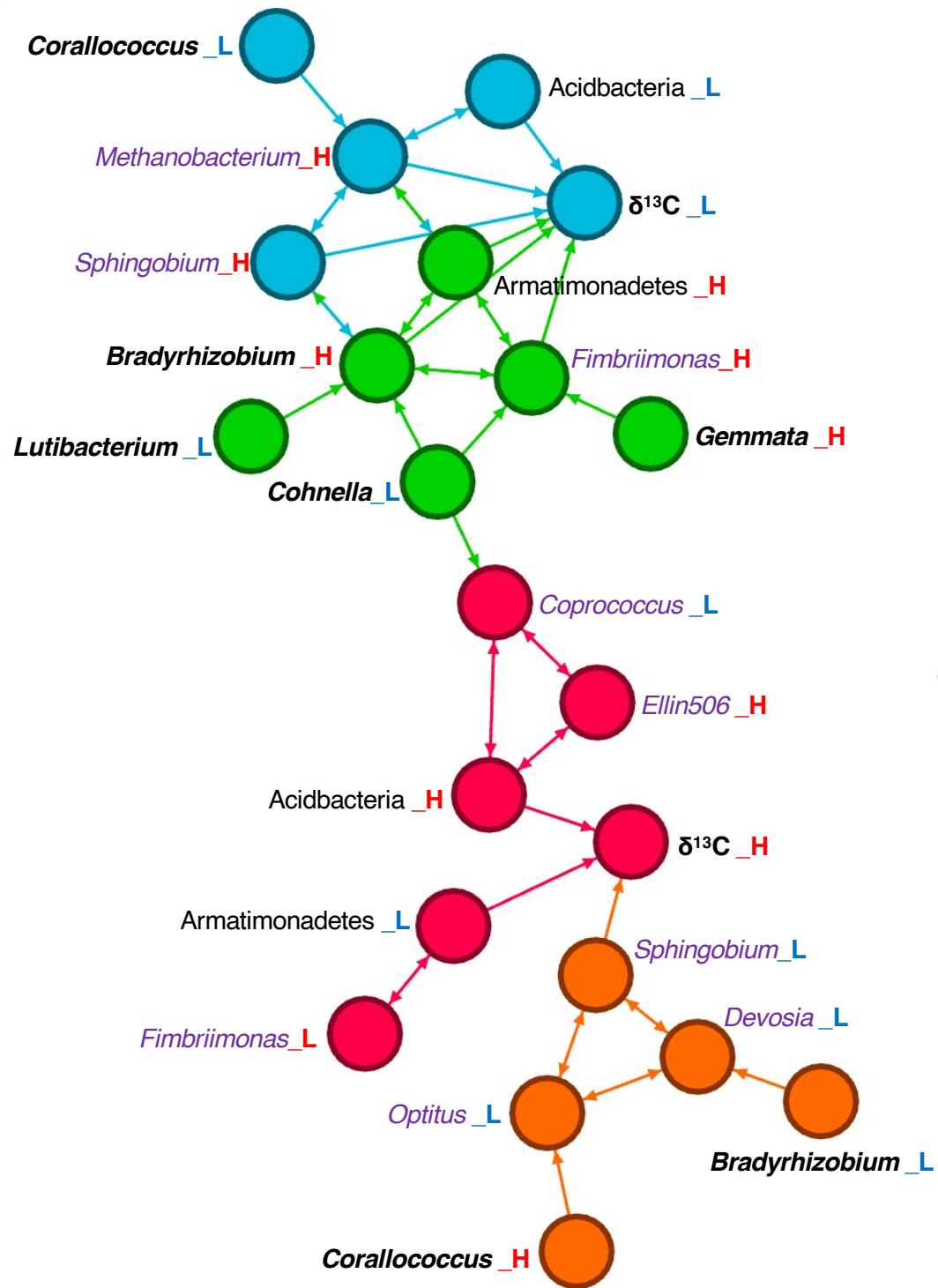
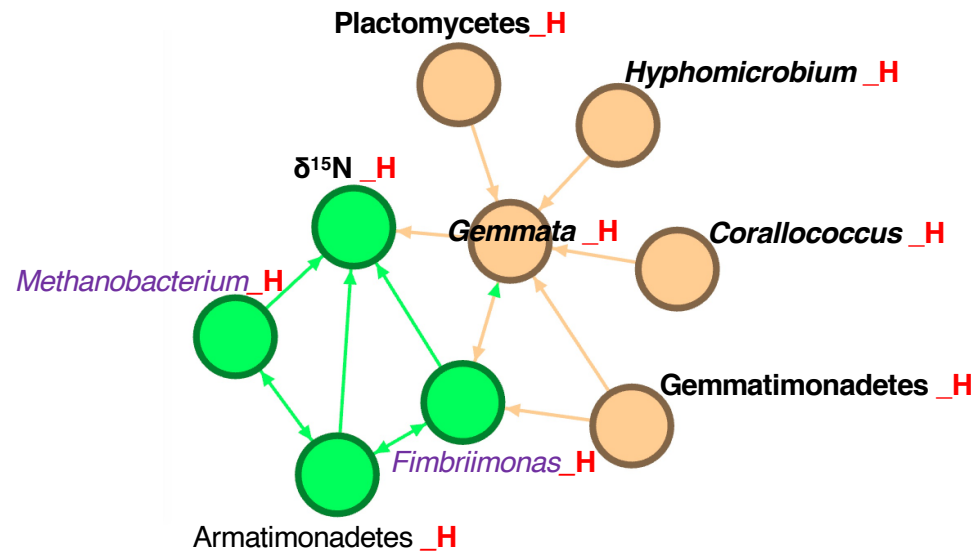


Fig.4

a



b



c

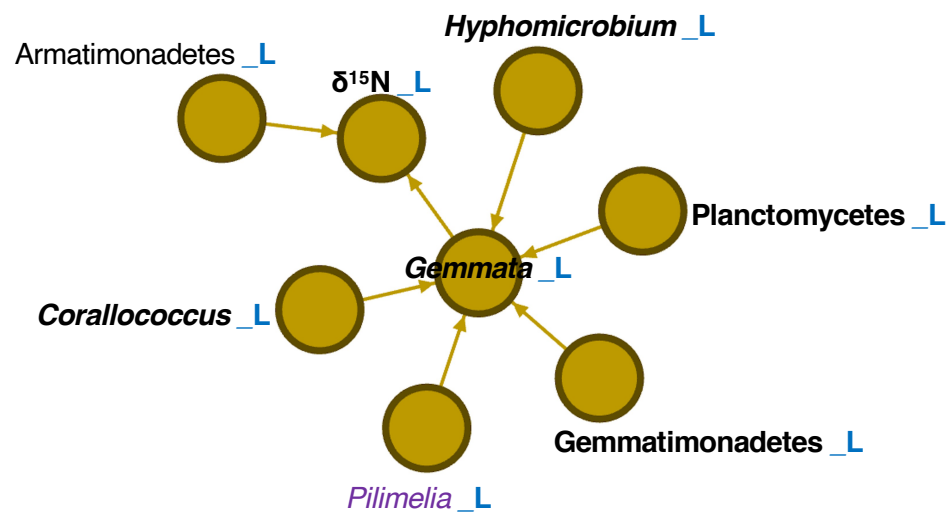


Fig.5

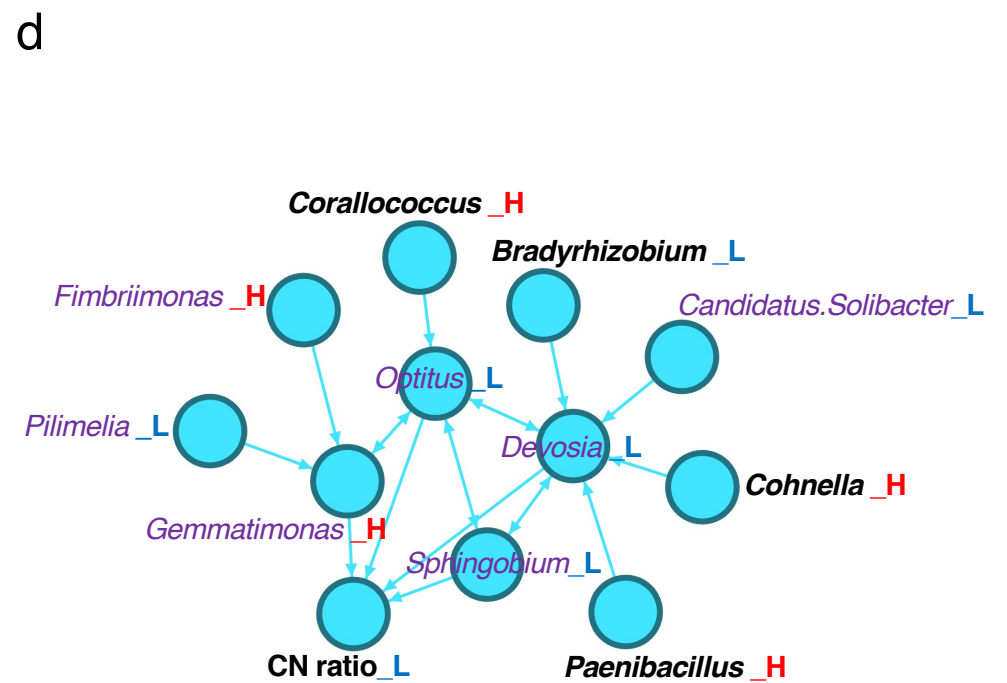
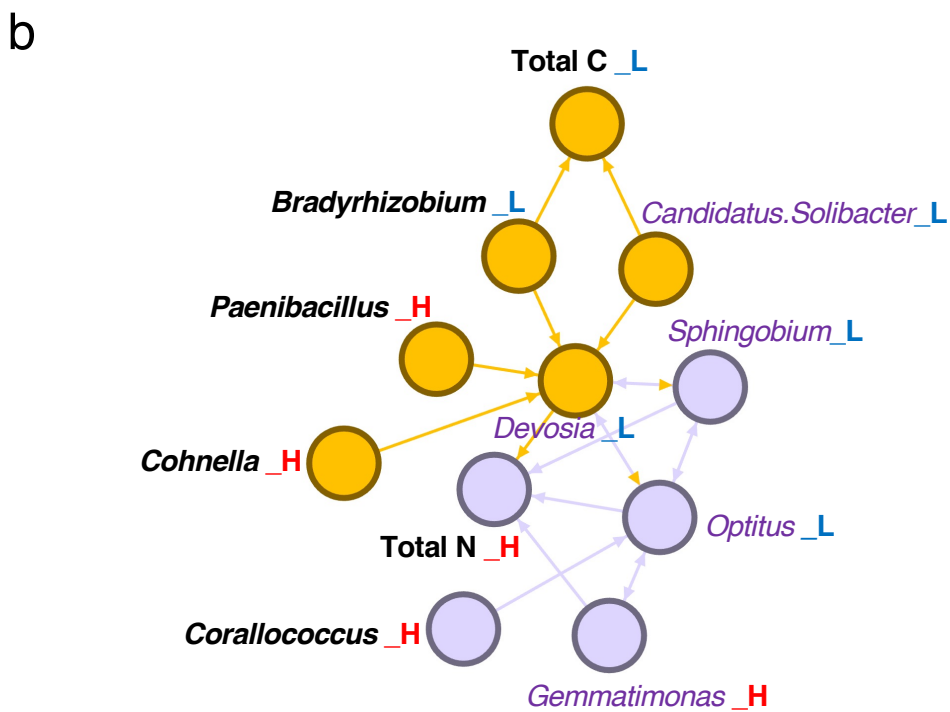
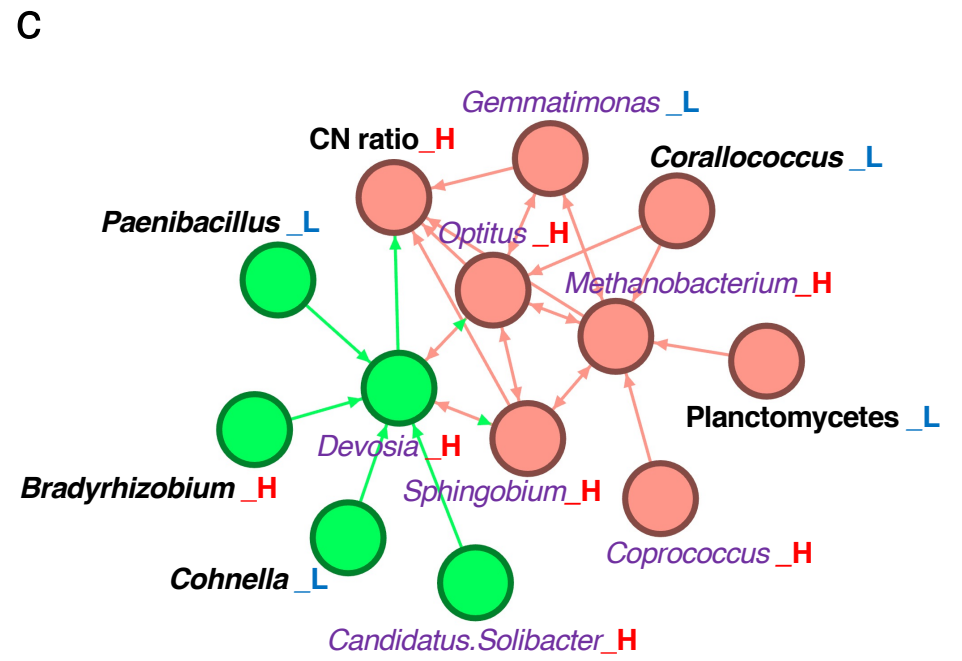
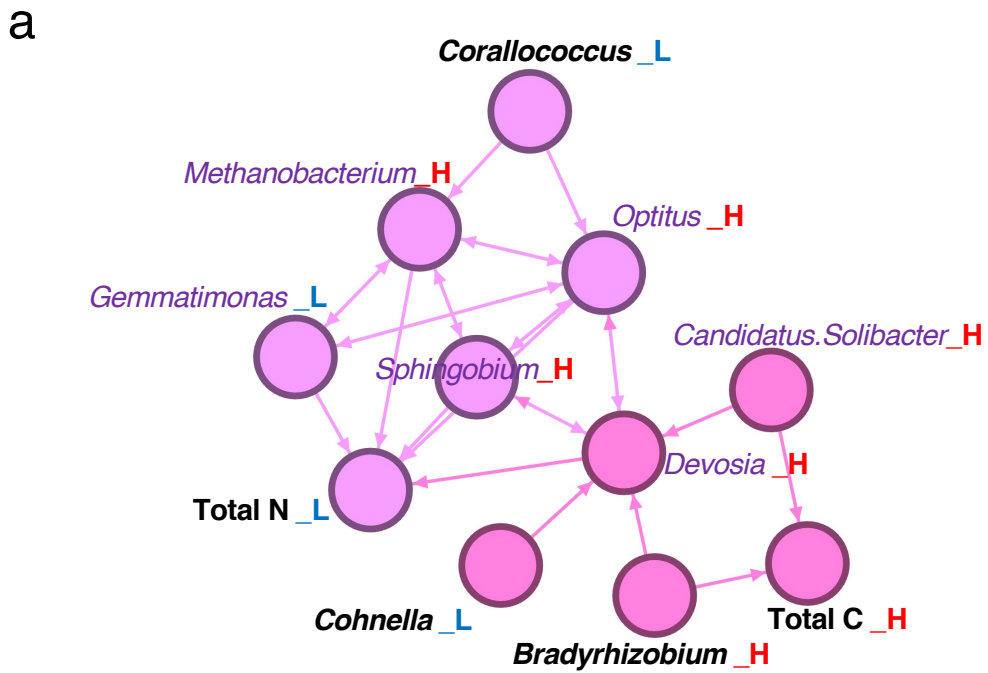


Fig.6

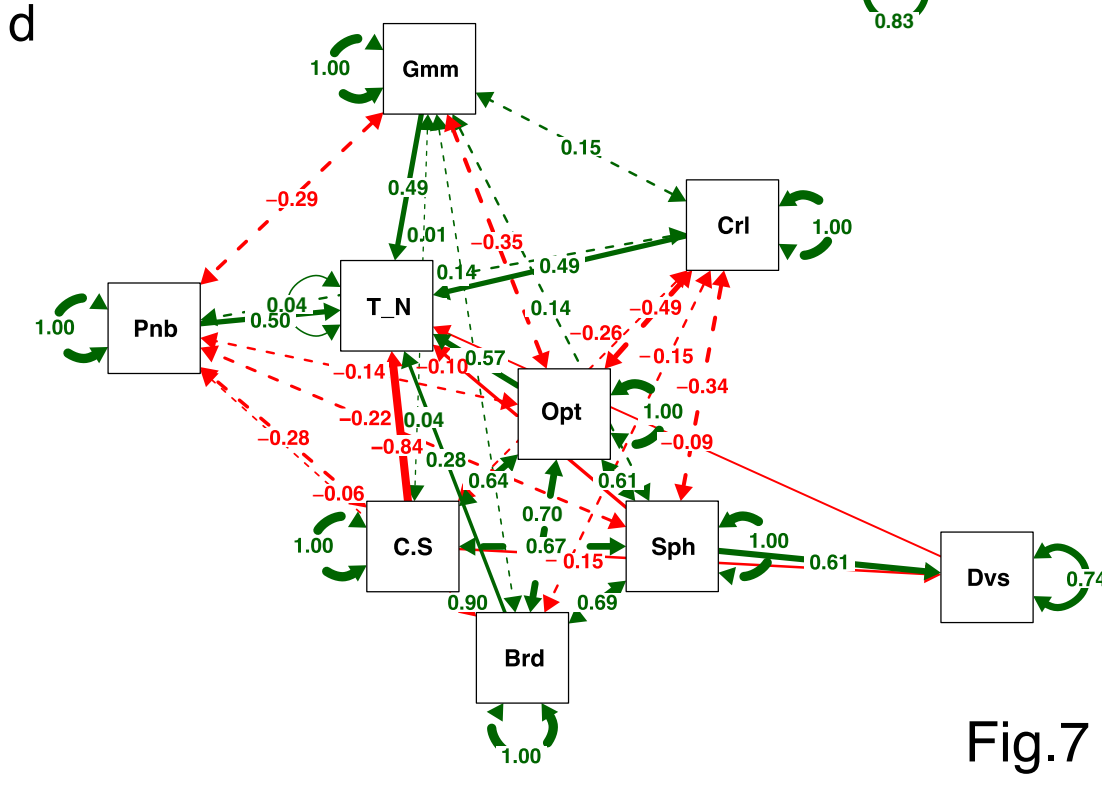
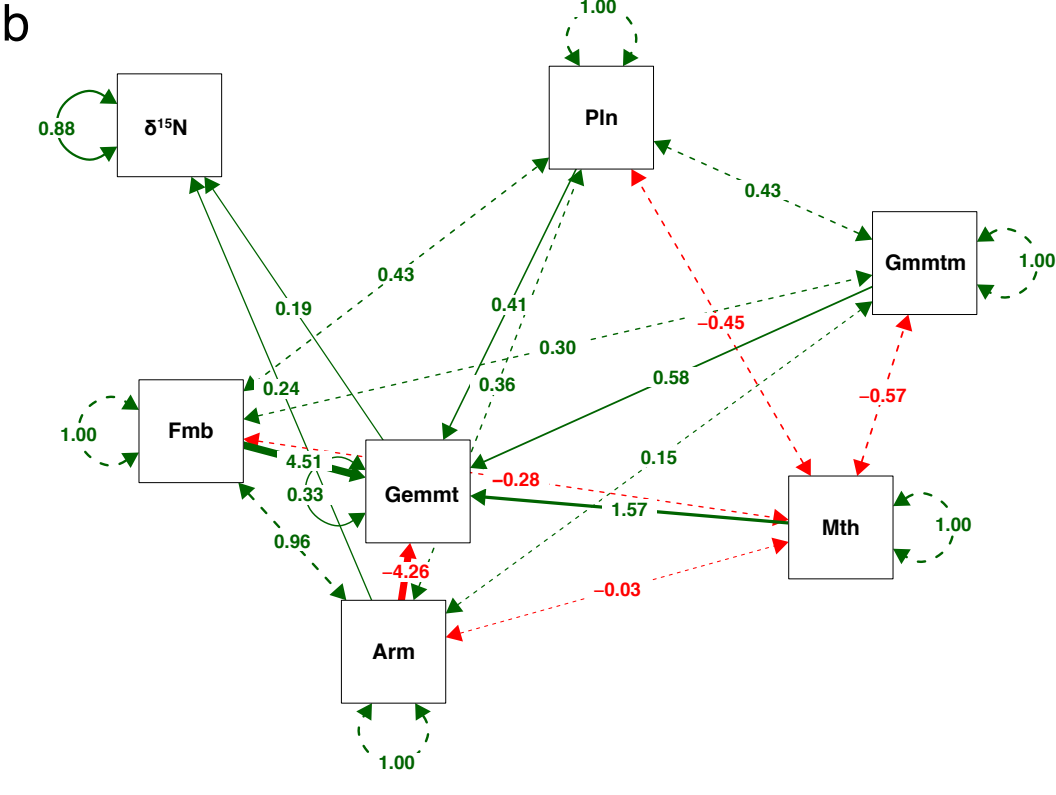
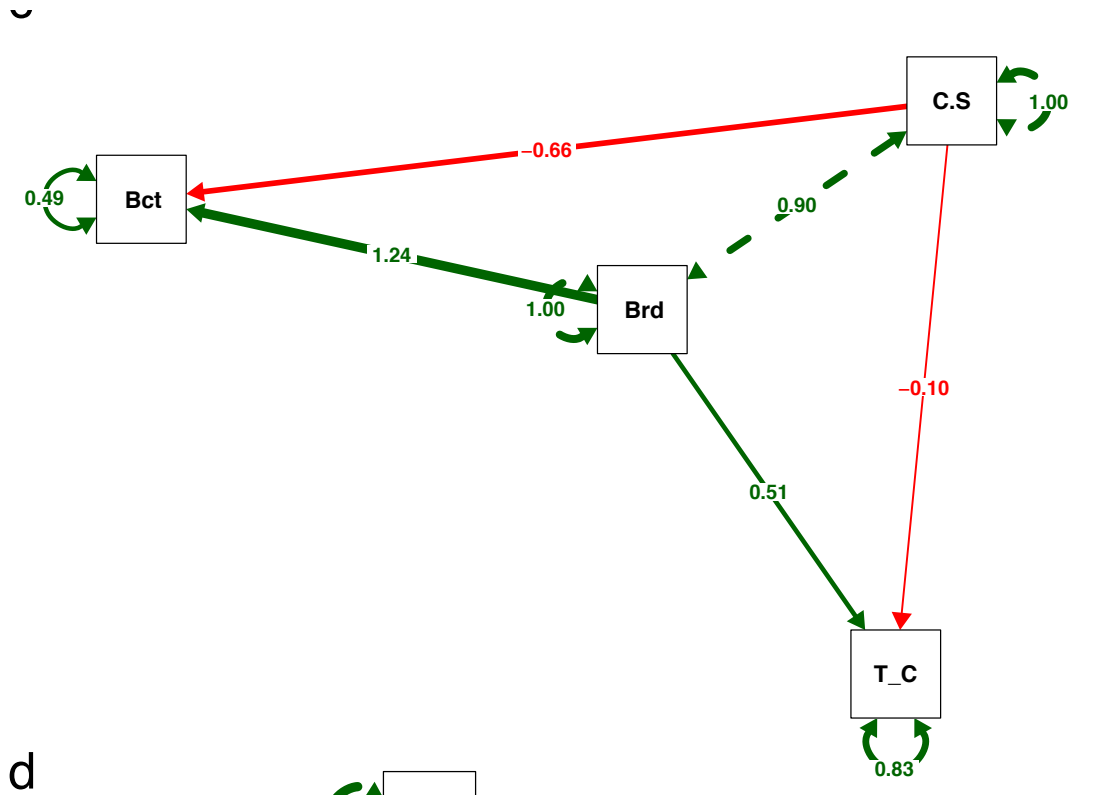
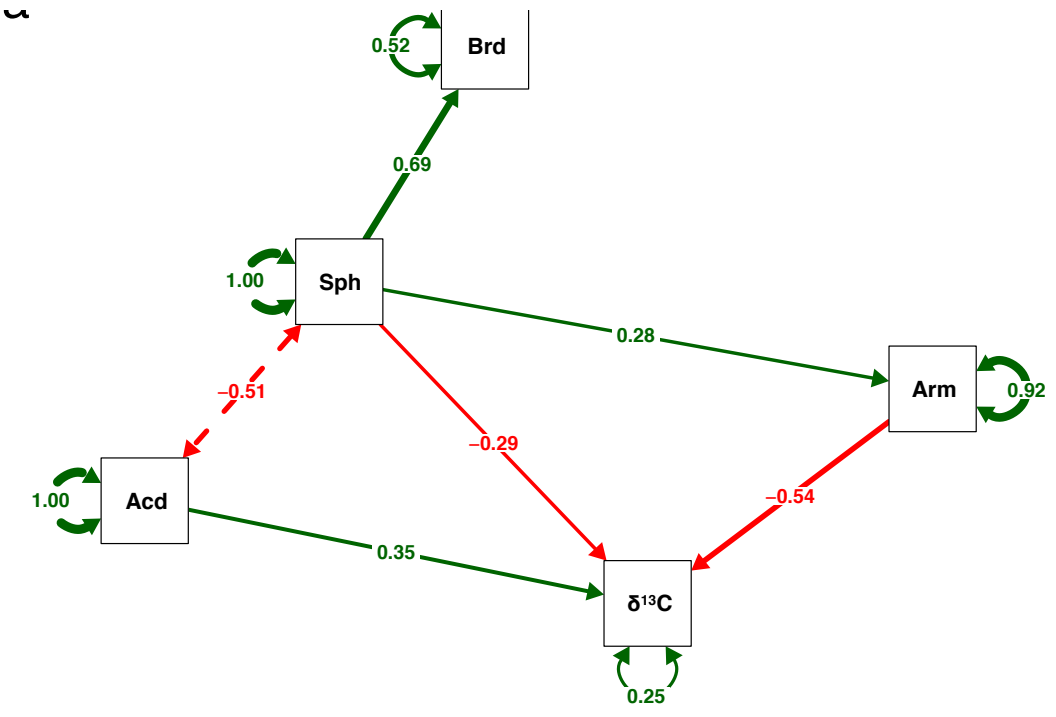


Fig.7

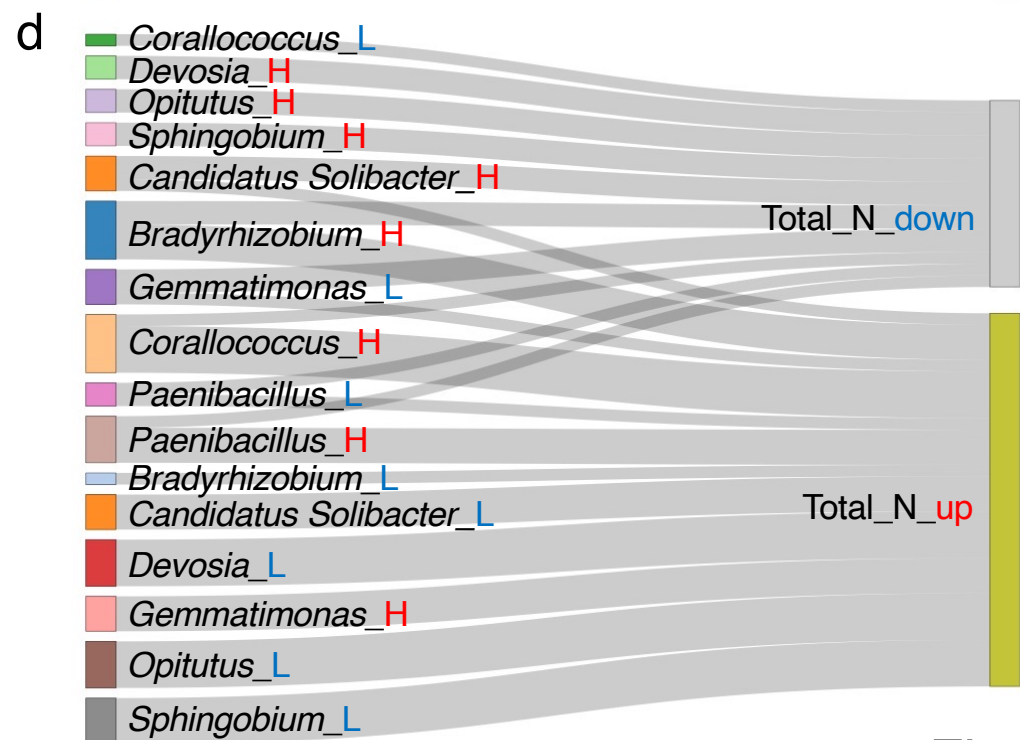
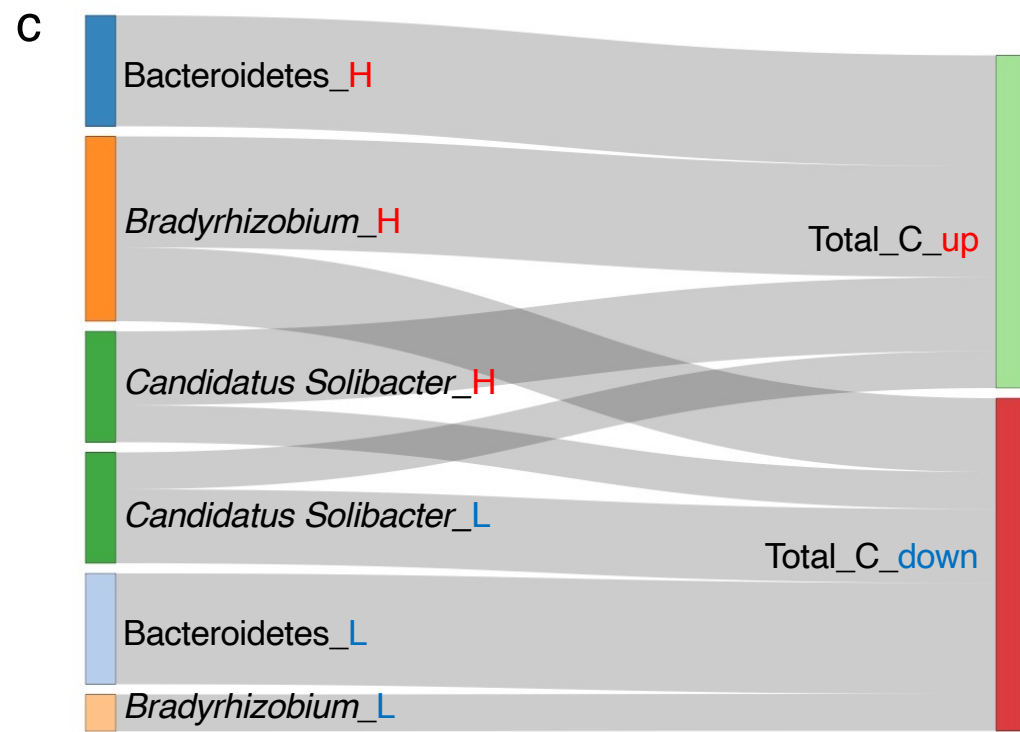
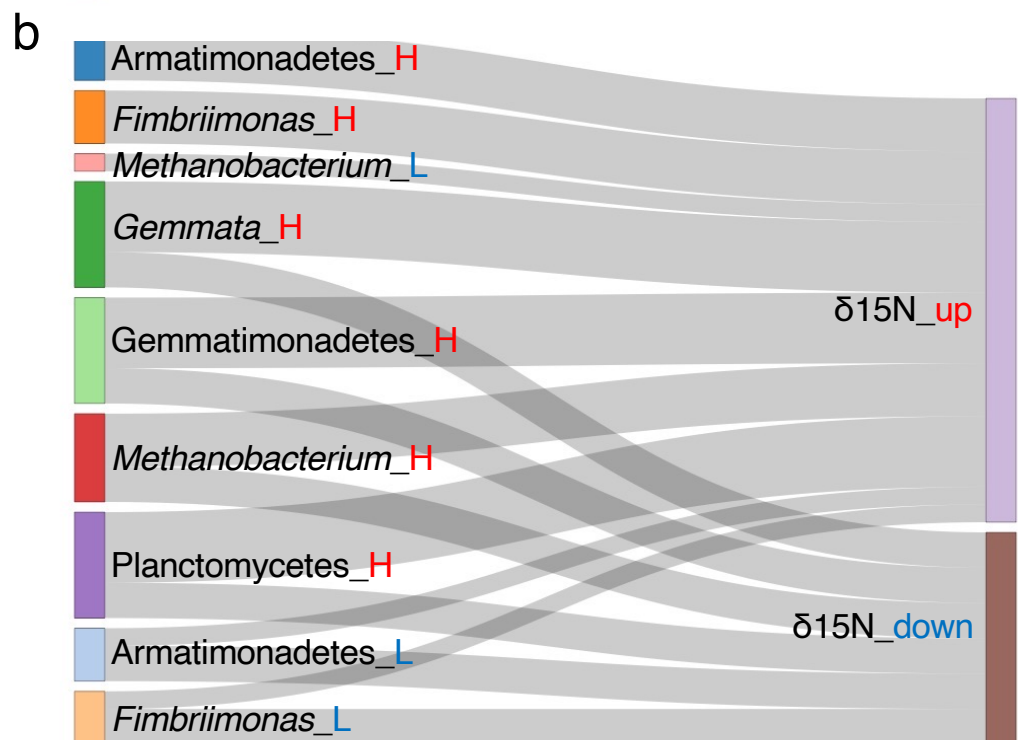
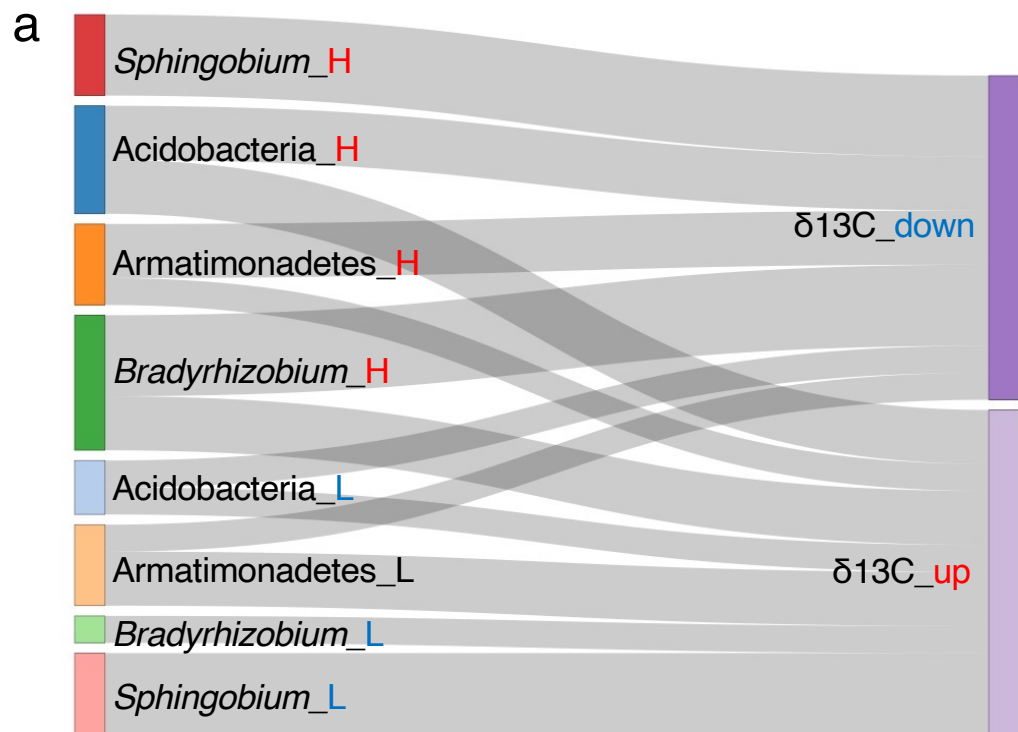
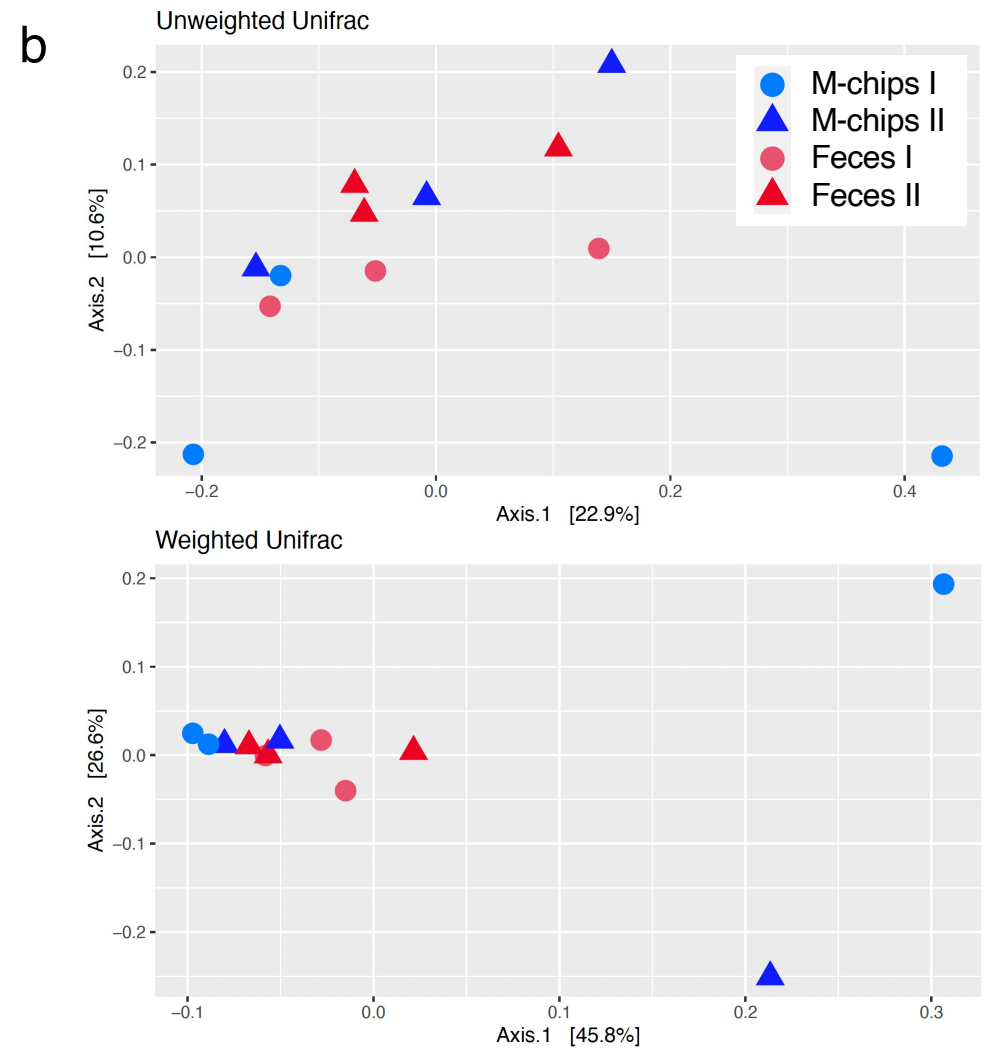
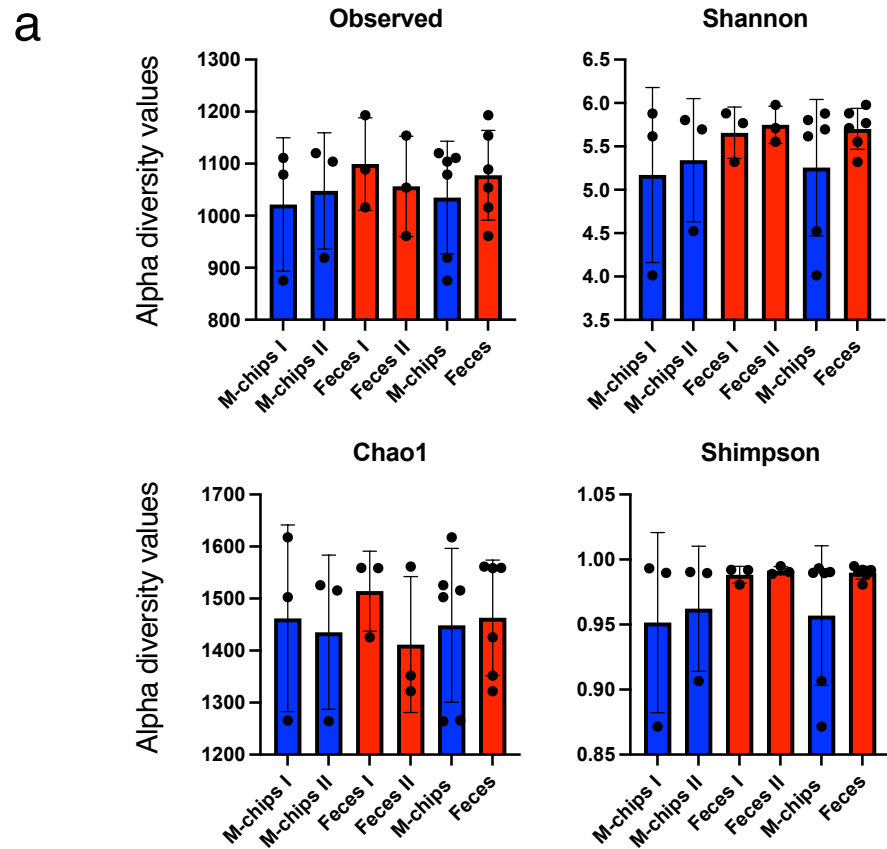


Fig.8



c

Category	No. subject	Unweigthed UniFrac		Weigthed UniFrac	
		R ²	P value	R ²	P value
M_chips I vs M_chips II	3 vs 3	0.18471	0.5	0.11703	0.9
Feces I vs Feces II	3 vs 3	0.18723	0.7	0.13263	0.9
M_chips vs Feces	6 vs 6	0.08184	0.727	0.07593	0.561

Fig. S1
 (a) OTU number and the Chao1, Shannon, and Simpson indices representing α -diversity in the habitat (M-chips) and feces (Feces). (b) UniFrac graph, unweighted and weighted, which shows β -diversities in the habitat (M-chips) and feces. (c) Values calculated based on unweighted and weighted data are shown under environmental conditions. I and II show environmental conditions: I, a group sprayed with water only; II, one sprayed with 20% compost extract.

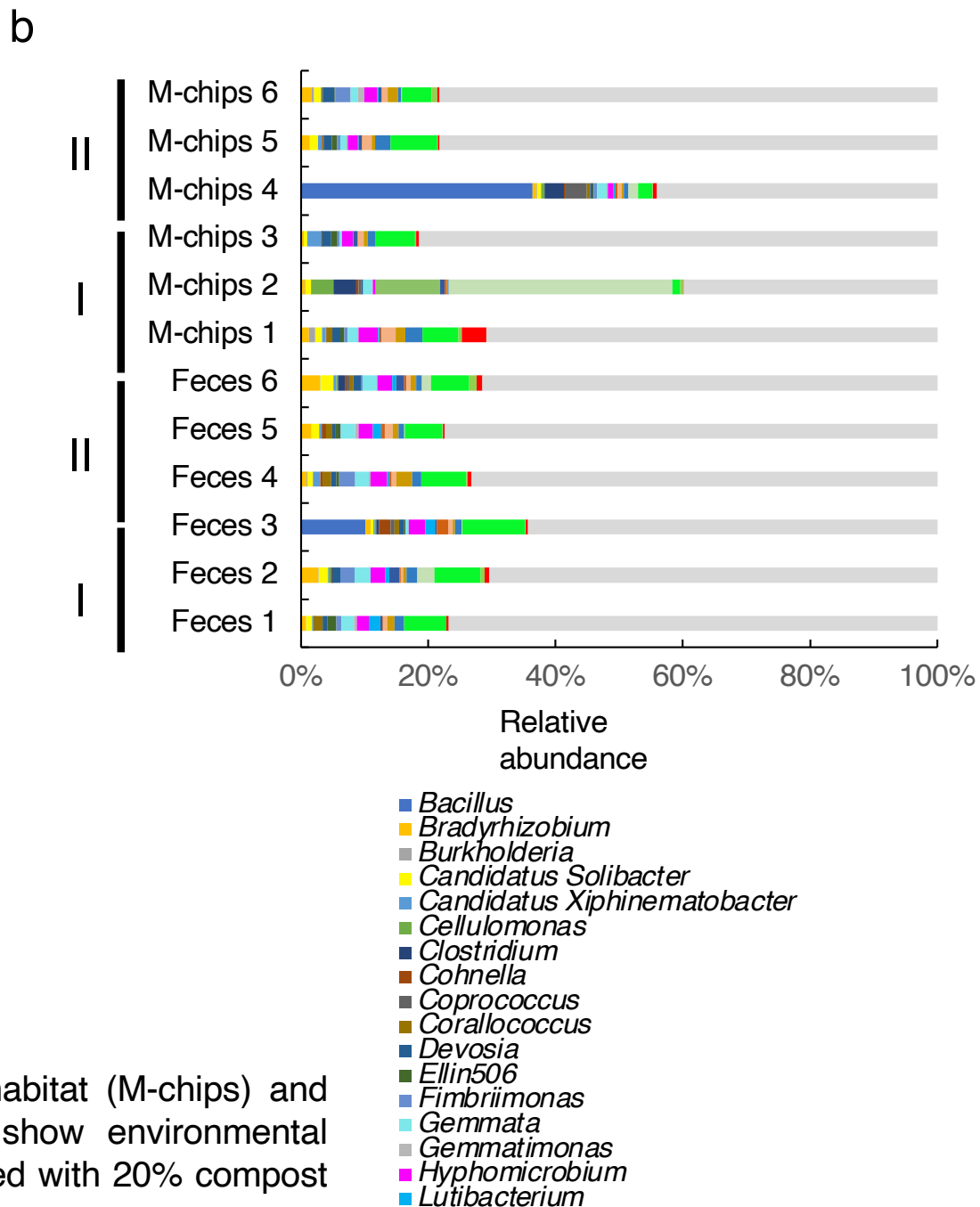
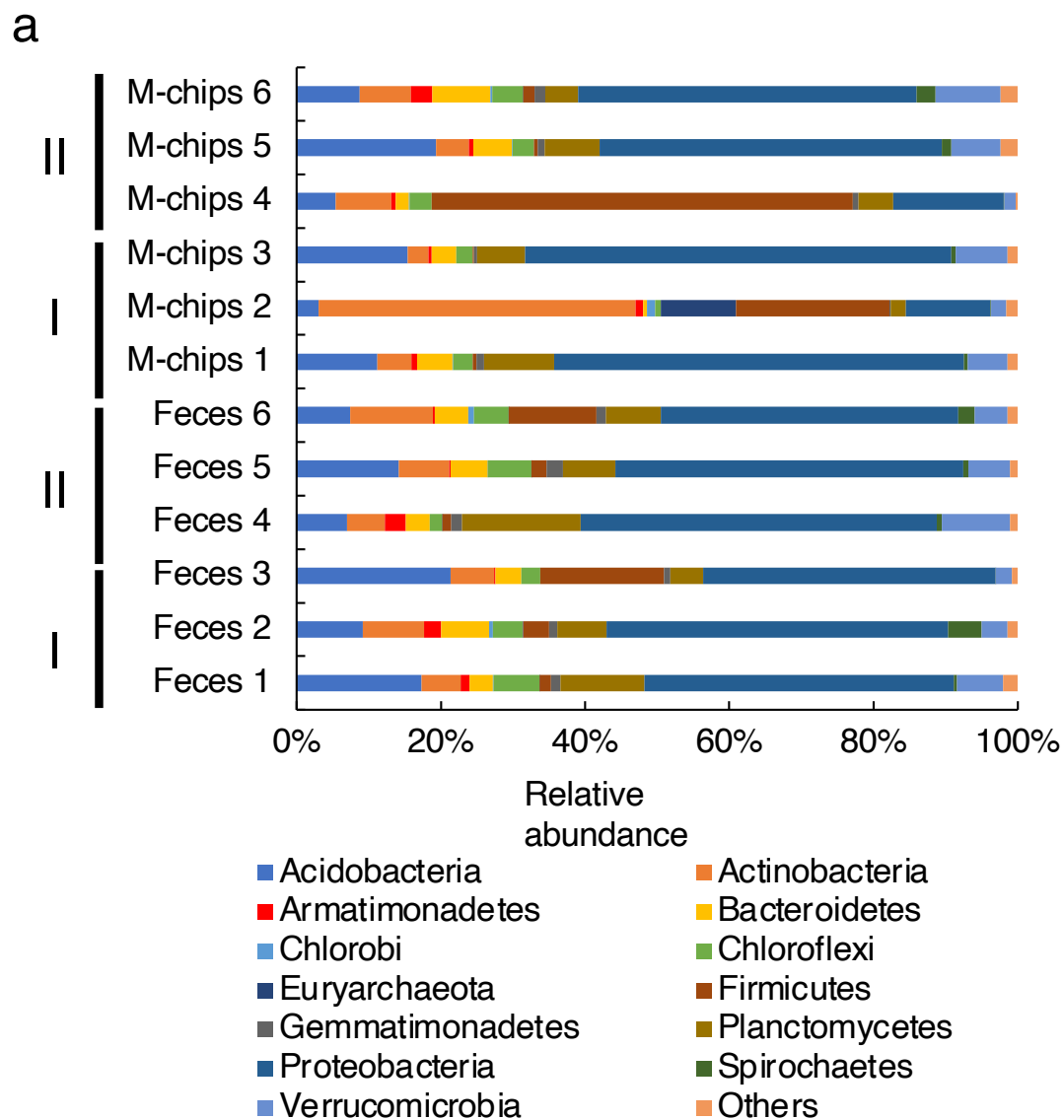
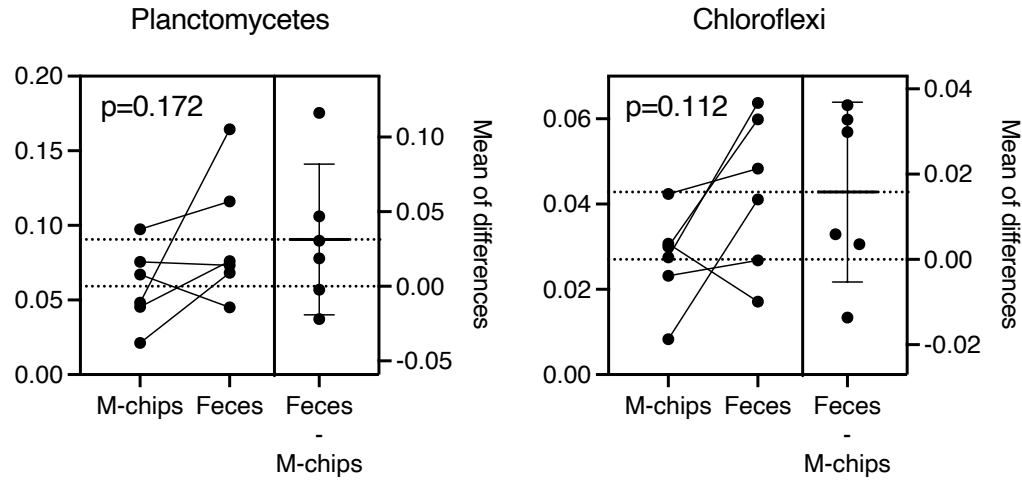
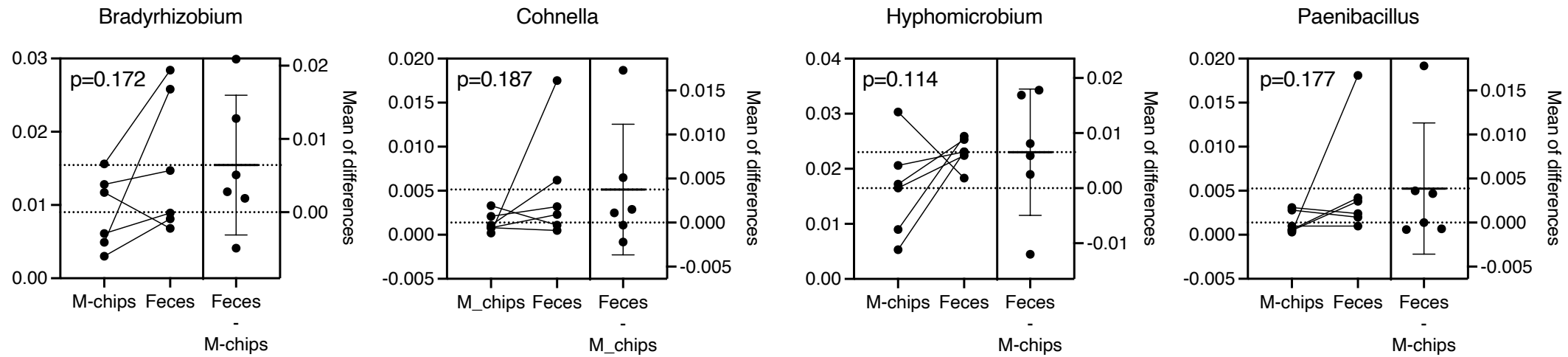


Fig. S2
 Relative abundances of (a) phyla and (b) genera in the habitat (M-chips) and feces (Feces) under environmental conditions. I and II show environmental conditions: I, a group sprayed with water only; II, one sprayed with 20% compost extract.

a**b****Fig. S3**

(a) Estimation plots of representative phyla and (b) genera in Fig. 2b with their significance values ($0.1 < p < 0.2$; $> 1\%$ as maximal value of the detected bacterial population among the whole population in each group).

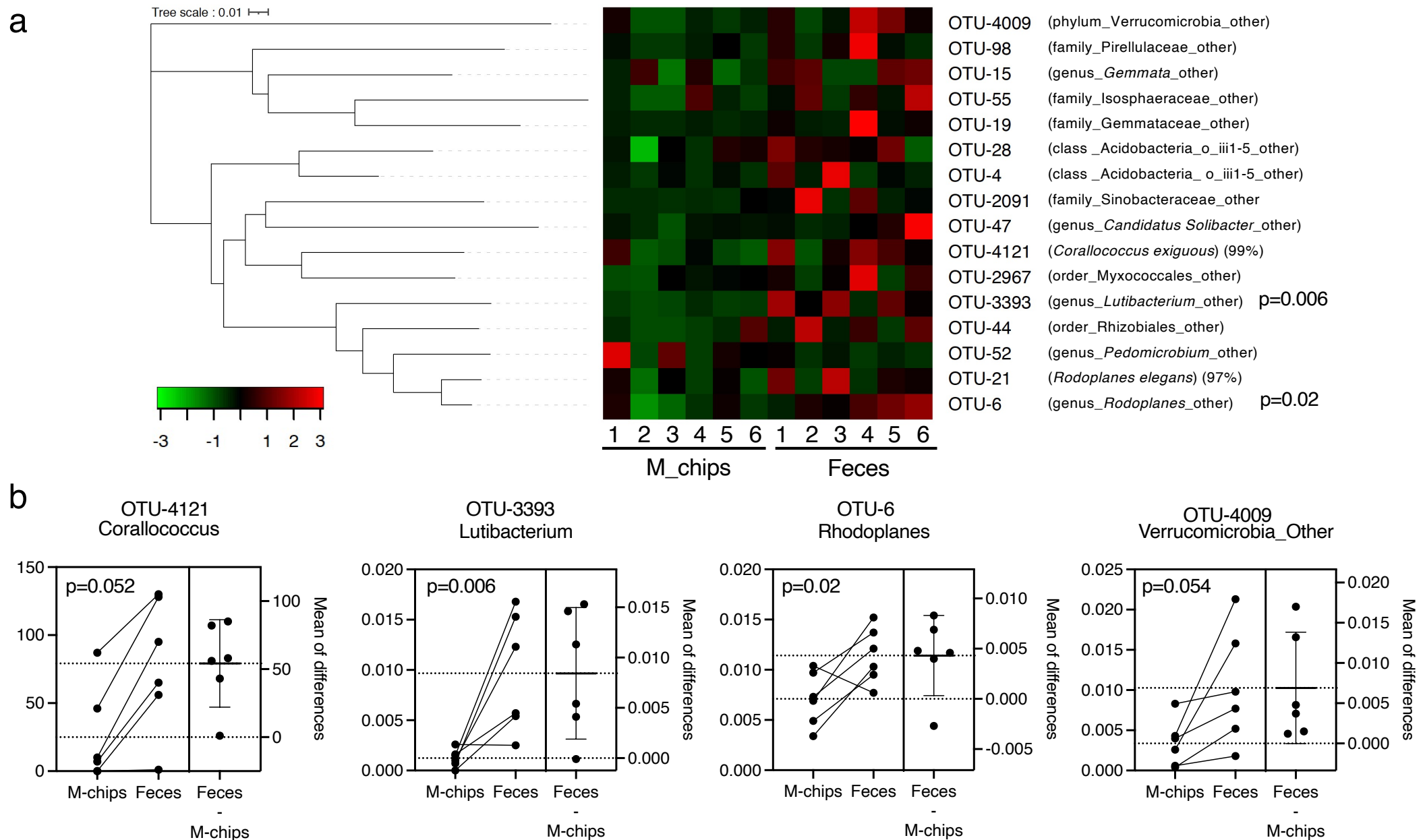


Fig. S4

(a) Phylogenetic tree and heatmap of representative bacterial OTUs in the feces ($p < 0.2$; $> 1\%$ as maximal value of the detected bacterial population among the whole population in each group).

(b) Estimation plots of representative OTUs in Fig. 3a with their significance values ($p < 0.1$; $> 1\%$ as maximal value of the detected bacterial population among the whole population in each group).

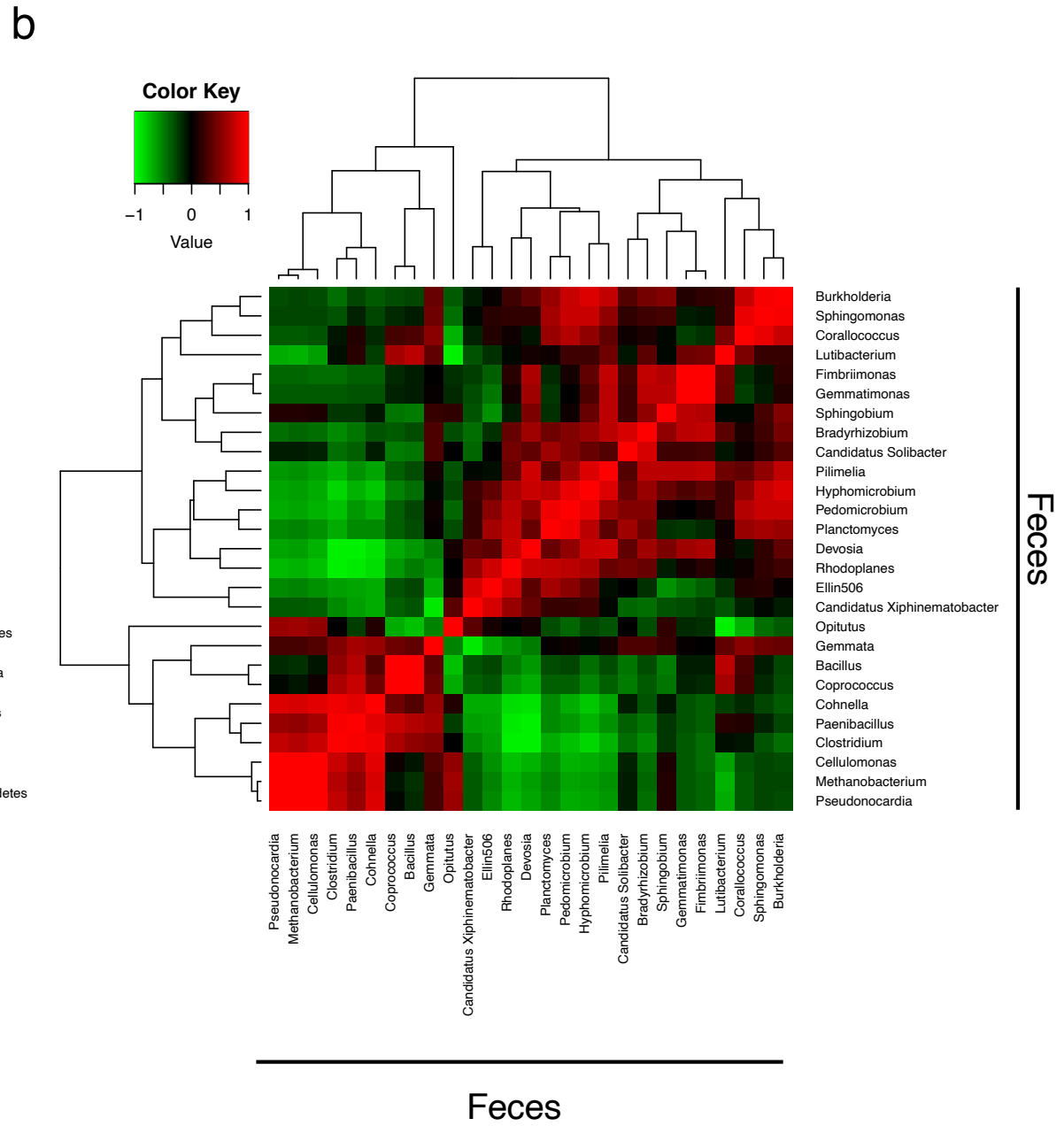
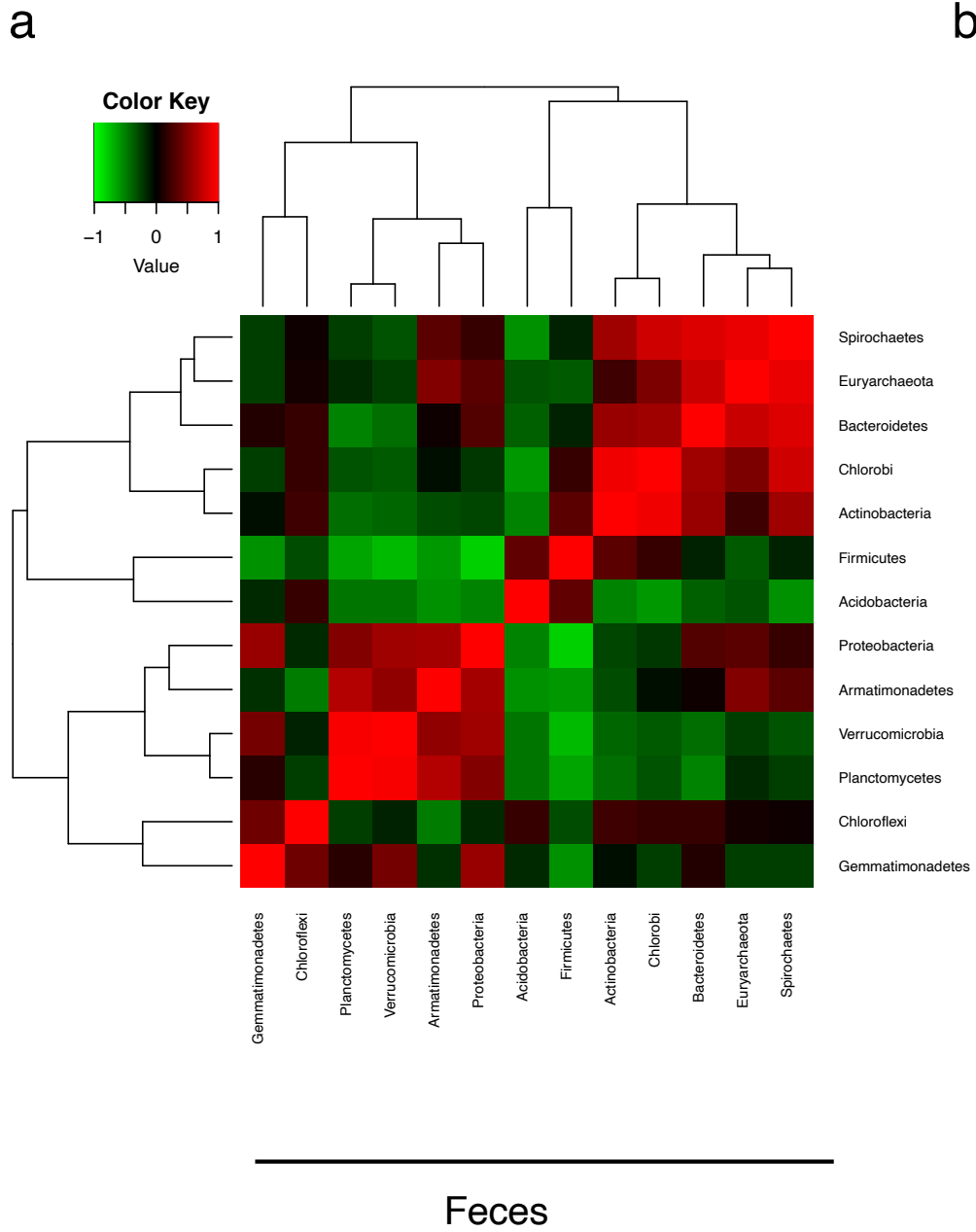


Fig. S5
Correlation heatmaps of the bacterial community in the feces of beetle larvae: (a) phyla and (b) genera.

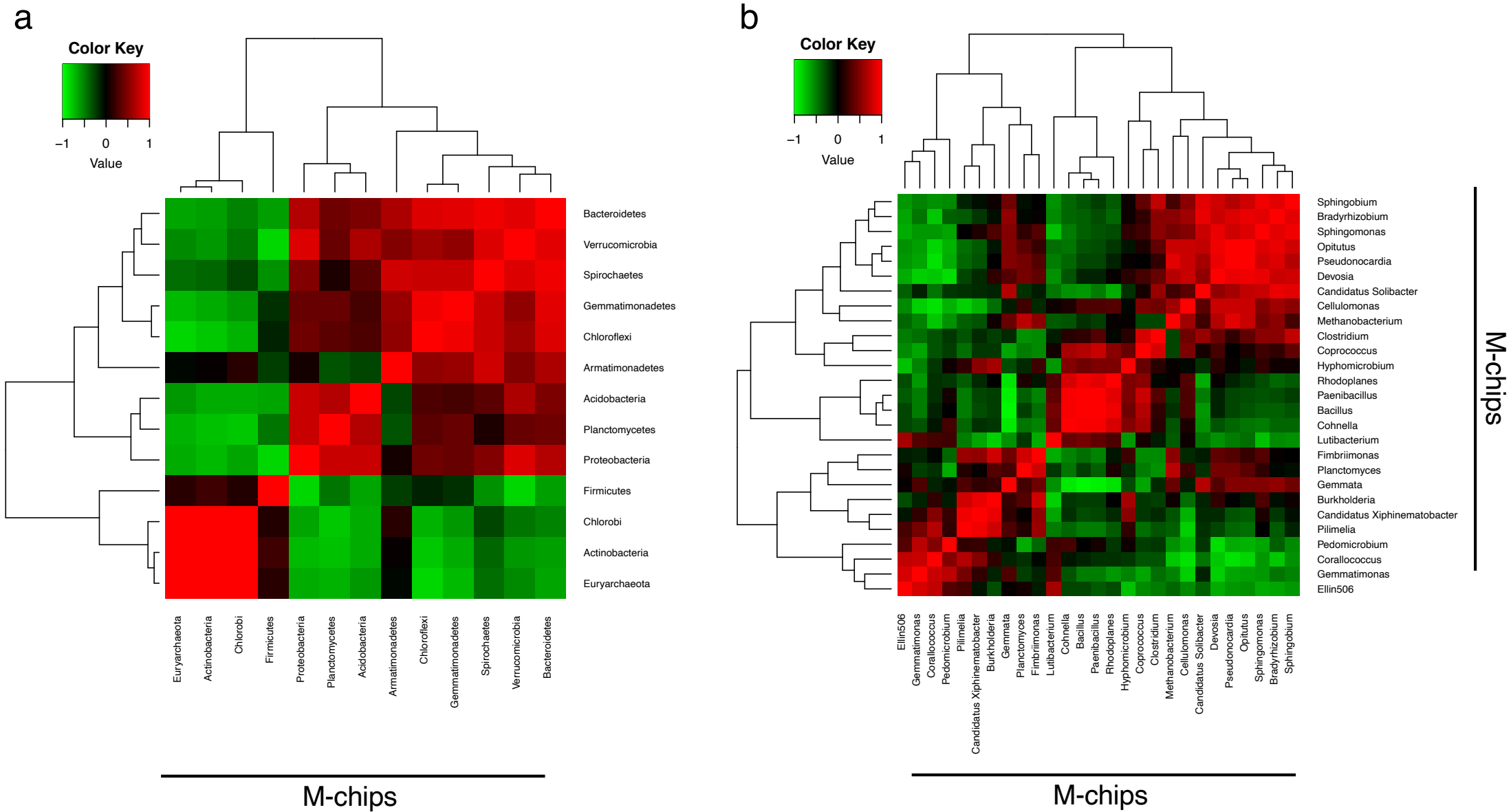


Fig. S6

Correlation heatmaps of the bacterial community in the habitat of beetle larvae alone (a) phyla and (b) genera

a



b

Component	Raw-Chips (3)	M-Chips			Feces		
		Condition I (3)	Condition II (3)	Total (6)	I (3)	II (3)	Total (6)
$\delta^{13}\text{C}$	-27.39 ± 0.01	-27.85 ± 0.04	-27.82 ± 0.15	-27.85 ± 0.04^b	-27.63 ± 0.15	-27.86 ± 0.12	-27.75 ± 0.10^c
$\delta^{15}\text{N}$	-2.92 ± 0.08	1.45 ± 0.06	0.77 ± 0.07^a	1.11 ± 0.16^b	1.83 ± 0.22	1.33 ± 0.61	1.58 ± 0.31^c
Total C (%)	47.81 ± 0.10	40.68 ± 2.90	44.01 ± 1.76	42.34 ± 1.69^b	42.48 ± 0.85	43.69 ± 1.14	43.08 ± 0.69^c
Total N (%)	0.34 ± 0.01	1.16 ± 0.10	1.24 ± 0.27	1.20 ± 0.13^b	1.93 ± 0.34^d	1.44 ± 0.27	1.69 ± 0.22^{cd}
C/N ratio	142.5 ± 2.34	35.48 ± 2.97	40.26 ± 11.3	37.87 ± 5.35^b	23.82 ± 5.24	33.34 ± 8.5	28.59 ± 4.95^c

Fig. S7

Photographs of the samples used in this experiment (a) and stable isotope ($\delta^{13}\text{C}$ and $\delta^{15}\text{N}$) levels, carbon, and nitrogen levels and carbon/nitrogen ratios in the fresh wood chips of the habitat (raw chips), the decayed chips (M-chips), and larval feces (Feces). I and II show environmental conditions: I, a group sprayed with water only; II, one sprayed with 20% compost extract.

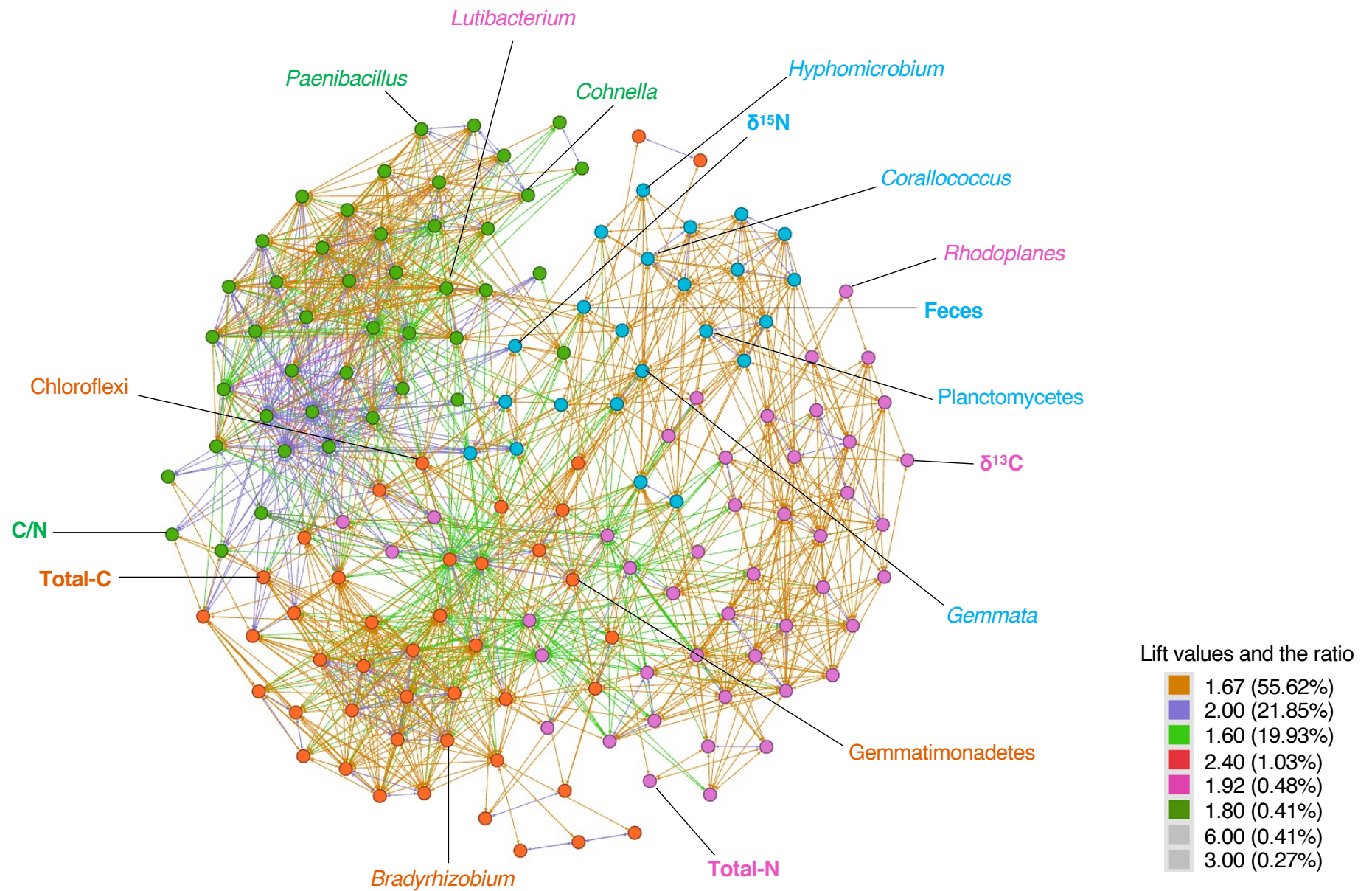


Fig. S8

Systemic networks of factors associated with chemical indices and feces. The factors shown in Figs. 2b and 6a are indicated with black lines. Modularity classes are discriminated by four colors, and lift values and the ratio are shown.

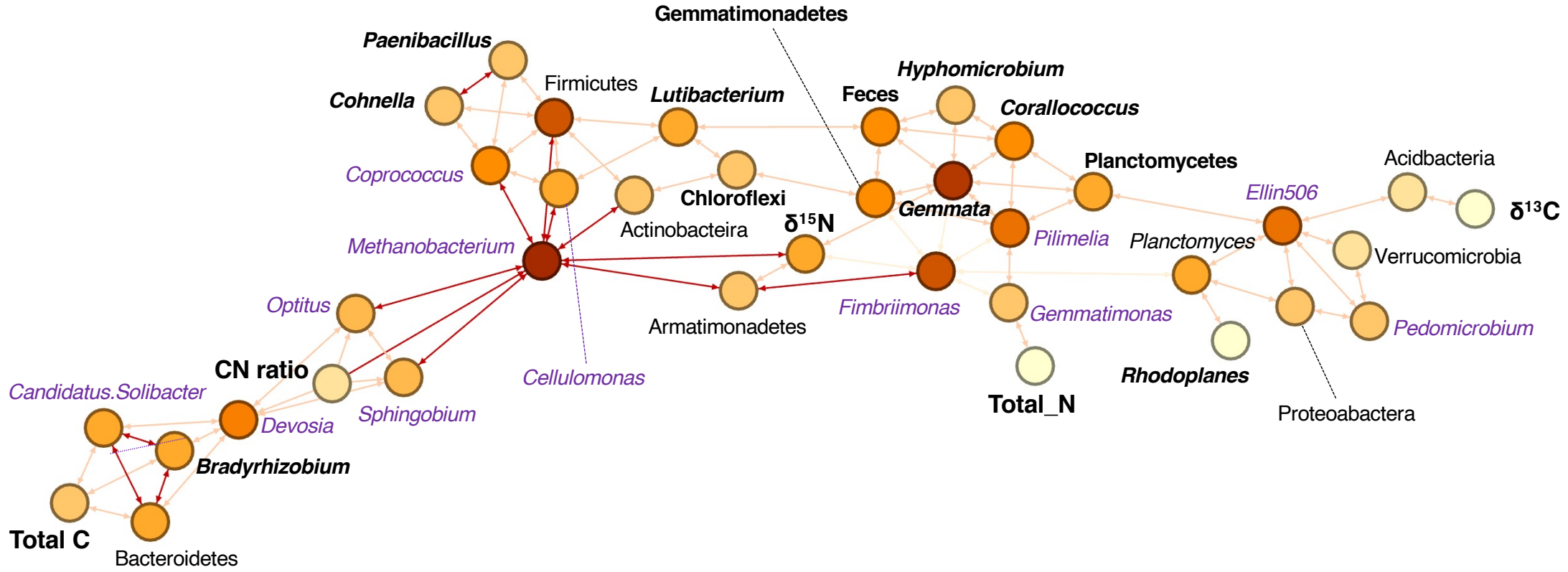


Fig. S9
 Systemic networks of factors shown in Figs. 2b and 6a. The difference of color of nodes indicates strength of degree, whose value sums up the weights of the adjacent edges for each node. The bacteria and components in Figs. 2b and 6a are shown in bold letters. Stable bacteria, the population of which was not significantly different between the habitat and the feces (Fig. S10), are shown in violet.

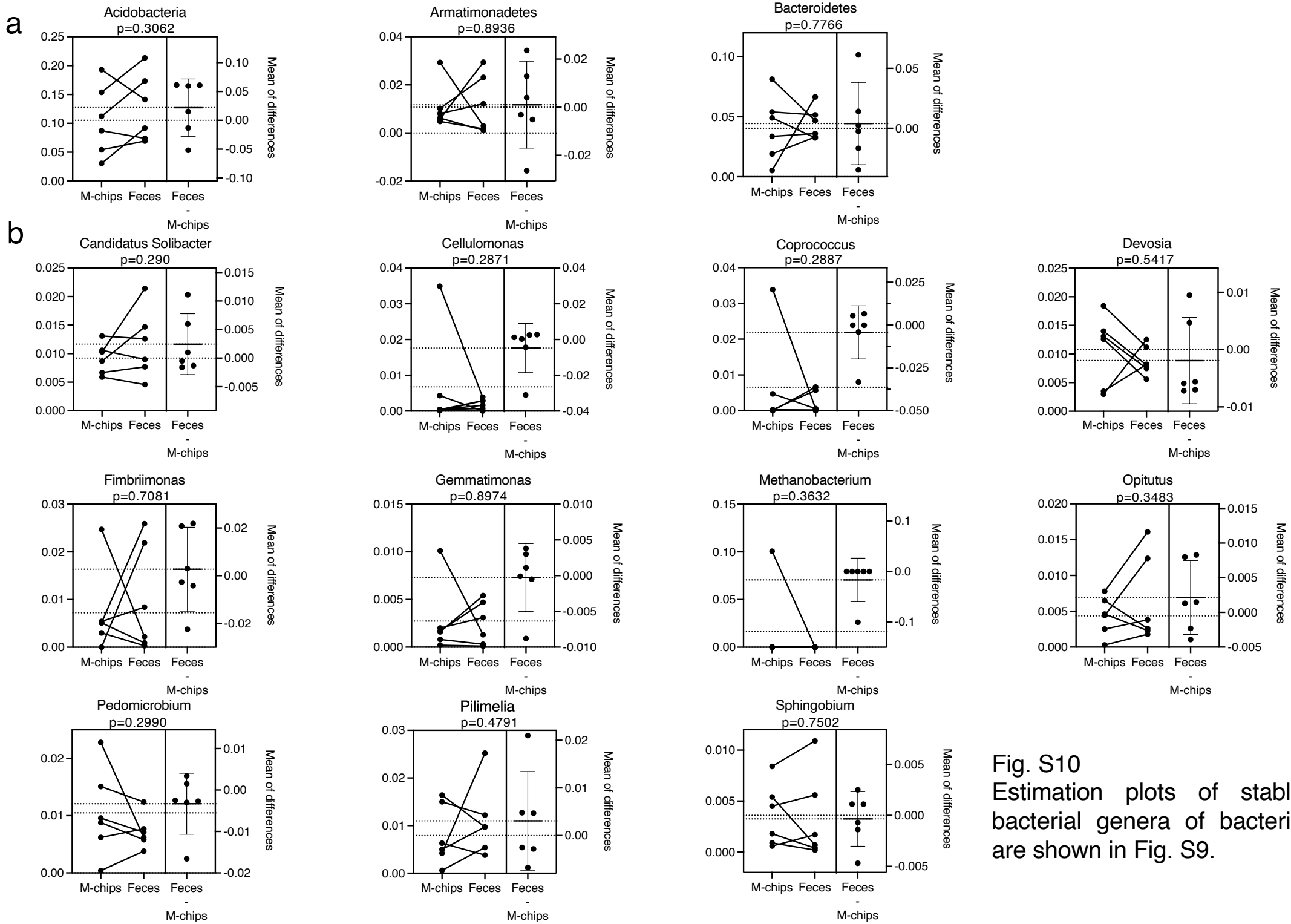


Fig. S10
 Estimation plots of stable bacterial genera of bacteria are shown in Fig. S9.

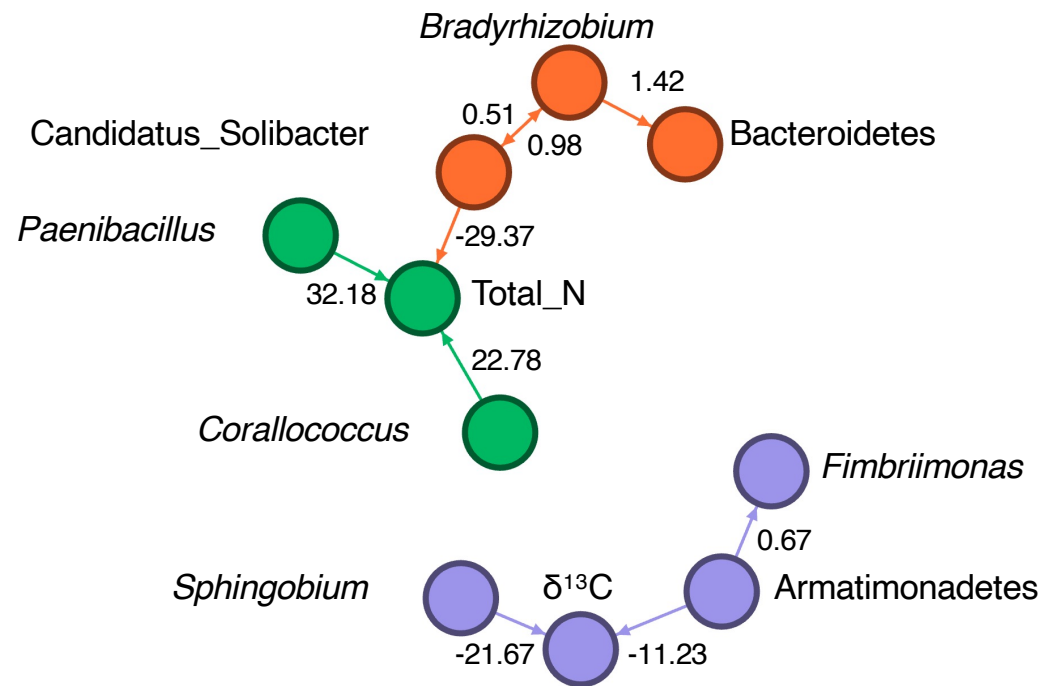
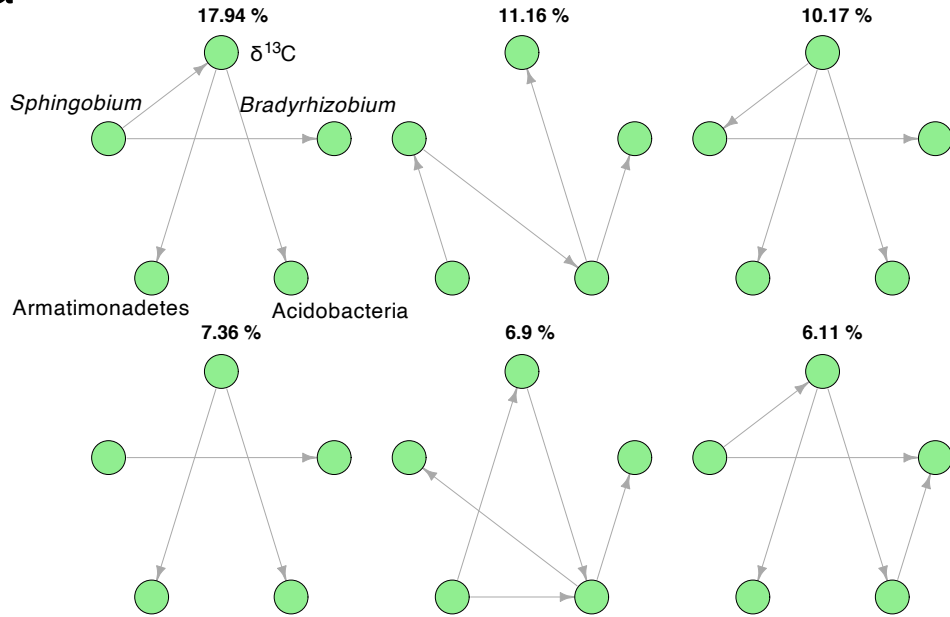
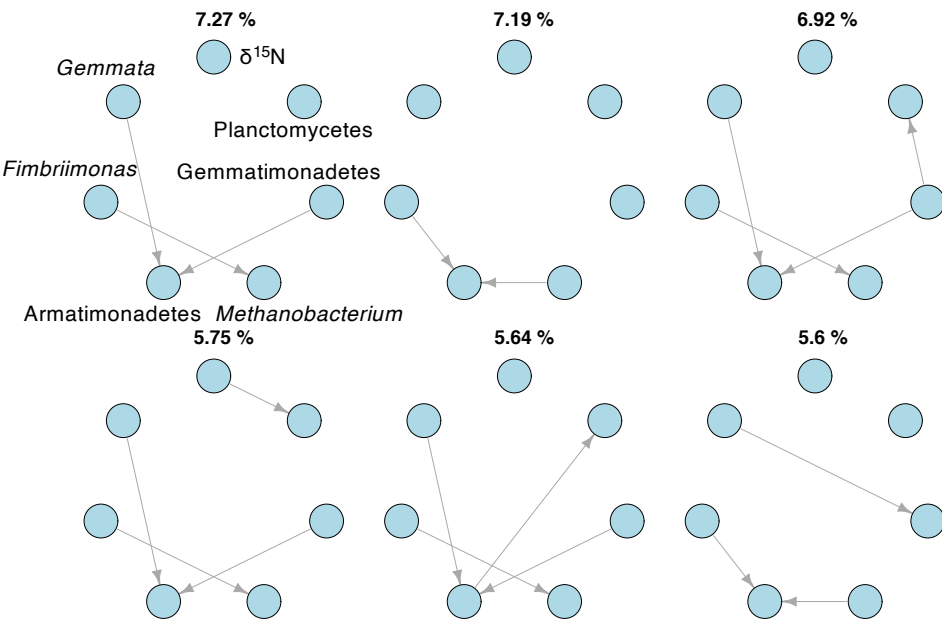
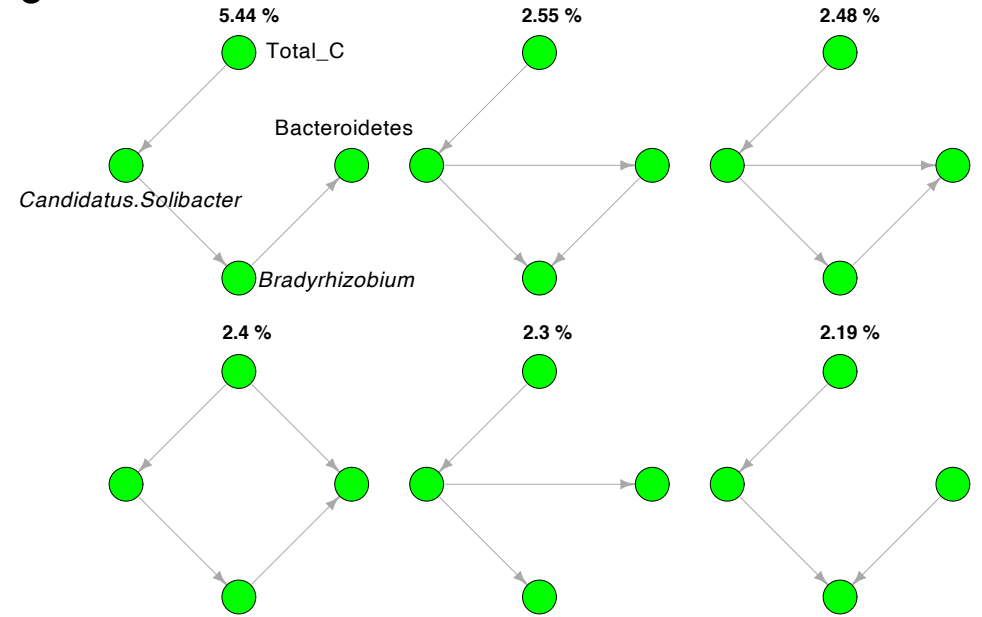
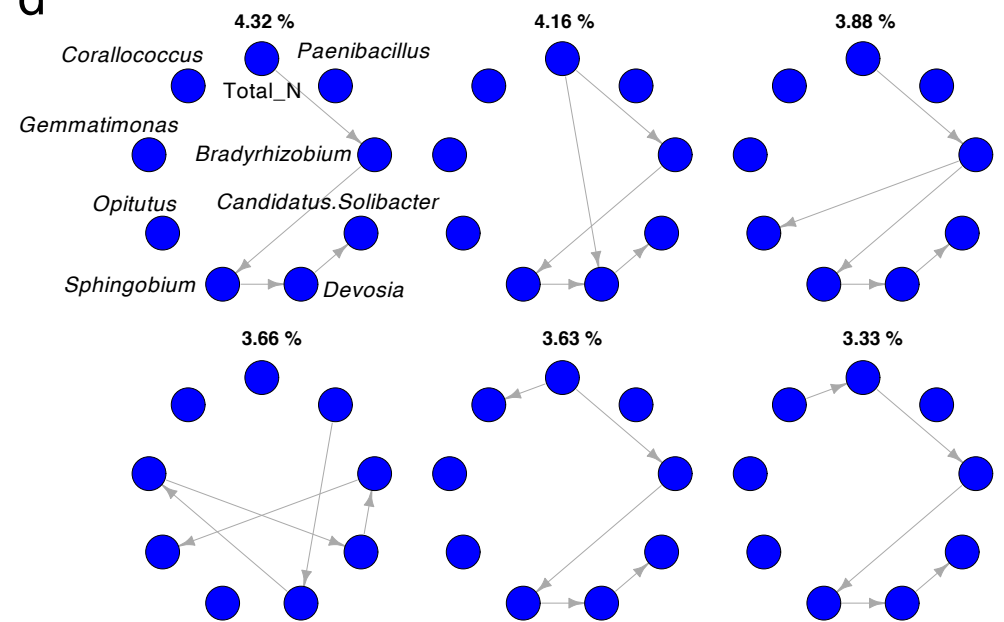


Fig. S11
 Causal relationship estimated by LiNGAM. The LiNGAM values shows the extents of contribution.

a**b****c****d****Fig. S12**

The top six groups composed by SEM estimated by BayesLiNGAM were visualized with percentages. The best appropriate groups calculated by SEM based on mediation values (M-chips and feces) in Fig. 7 were selected.

Table S1.

Body weights of larvae used in this experiment. One male larva and one female larva were bred in the same box for one month. I and II show environmental conditions: I, a group sprayed with water only; II, one sprayed with 20% compost extract

Condition	Category	Body weight of larvae (g)				
		2018/5/6	2018/5/20	2018/5/27	2018/6/9	
I	Box 1	male	22	22	24	21
		female	19	19	18	16
	Box 2	male	23	23	17	27
		female	19	19	22	19
	Box 3	male	21	21	20	18
		female	17	17	17	17
	Box 4	male	20	20	20	20
		female	17	17	18	19
II	Box 5	male	25	25	27	17
		female	14	14	14	11
	Box 6	male	22	22	22	17
		female	17	17	18	17

↑
plus New chips

Table S2.

Statistical values of the final optimal structural equation models for $\delta^{13}\text{C}$, $\delta^{15}\text{N}$, total carbon, and total nitrogen in Fig. 6. Short terms in the table mean as follows: chisq, chi-square χ^2 ; df, degrees of freedom; p value, p-values (chi-square); cfi, comparative fit index; tli, Tucker–Lewis index; nfi, normed fit index; rfi, relative fit index; SRMR, standardized root mean residuals; AIC, Akaike information criterion; rmsea, root mean square error of approximation ; gfi, goodness-of-fit index; agfi, adjusted goodness-of-fit index. The No.1 column shows the best numerical structural equation model for $\delta^{13}\text{C}$, $\delta^{15}\text{N}$, total carbon, and total nitrogen, respectively. The No.2 column shows the inferior numerical structural equation models.

Category	No.1			No.2			
$\delta^{13}\text{C}$	Model	Delta13C ~ Sphingobium + Armatimonadetes + Acidobacteria			Delta13C ~ Sphingobium + Armatimonadetes		
		Bradyrhizobium + Armatimonadetes ~ Sphingobium			Armatimonadetes ~ Sphingobium		
	Fit indices	chisq 2.364 cfi 1.000 nfi 0.917 rmsea 0	df 4 tli 1.186 SRMR 0.0986 gfi 0.953	pvalue 0.669 rfi 0.815 AIC -175.37 agfi 0.823	chisq 1.220 cfi 985 nfi 0.939 rmsea 0.136	df 1 tli 0.926 SRMR 0.041 gfi 0.950	pvalue 0.269 rfi 0.693 AIC -88.580 agf 0.499
$\delta^{15}\text{N}$	Model	Delta15N ~ Gemmata			Delta15N ~ Gemmata		
		Gemmata ~ Fimbriimonas + Armatimonadetes + Methanobacterium			Gemmata ~ Fimbriimonas + Armatimonadetes + Methanobacterium		
		Gemmata ~ Gemmatimonadetes + Planctomycetes			Gemmata ~ Gemmatimonadetes		
Total C	Model	Delta15N ~ Armatimonadetes			Delta15N ~ Armatimonadetes		
		Total_C ~ Candidatus.Solibacter + Bradyrhizobium			Total_C ~ Candidatus.Solibacter + Bradyrhizobium		
		Bacteroidetes ~ Candidatus.Solibacter + Bradyrhizobium			Bradyrhizobium ~ Devosia		
Total N		Candidatus.Solibacter ~ Devosia			Candidatus.Solibacter ~ Devosia		
	Fit indices	chisq 0.051 cfi 1 nfi 0.996 rmsea 0	df 1 tli 1.533 SRMR 0.013 gfi 0.998	pvalue 0.822 rfi 0.982 AIC 0.640 agfi 0.975	chisq 19.289 cfi 0.051 nfi 0.203 rmsea 0.849	df 2 tli -1.848 SRMR 0.287 gfi 0.625	pvalue 6.48E-05 rfi 1 AIC -110.42 agfi -0.876
	Model	Total_N ~ Coralloccoccus + Gemmatimonas + Opiritutus + Sphingobium			Total_N ~ Coralloccoccus + Gemmatimonas + Opiritutus + Devosia		
Total N	Model	Total_N ~ Devosia + Candidatus.Solibacter + Bradyrhizobium + Paenibacillus			Total_N ~ Candidatus.Solibacter + Bradyrhizobium + Paenibacillus + Cohnella		
		Devosia ~ Candidatus.Solibacter + Sphingobium			Devosia ~ Candidatus.Solibacter		
	Fit indices	chisq 4.445 cfi 1 nfi 0.907 rmsea 0	df 5 tli 1.051 SRMR 0.055 gfi 0.999	pvalue 0.487 rfi 0.720 AIC -99.03 agfi 0.991	chisq 6.874 cfi 0.967 nfi 0.836 rmsea 0.110	df 6 tli 0.918 SRMR 0.090 gfi 0.996	pvalue 0.333 rfi 0.589 AIC -92.706 agfi 0.971

Table S3.

List of models targeted by causal mediation analysis (CMA) for $\delta^{13}\text{C}$ in Fig. 6 and their statistical values. Short terms in the table mean as follows: ACME, average causal mediation effects; ADE, the average direct effects.

$\delta^{13}\text{C}$ regression models						(I)Delta13C ~ Sphingobium + Armatimonadetes + Acidobacteria (II)Bradyrhizobium + Armatimonadetes ~ Sphingobium
(I)	Estimate	std. Error	t value	Pr (> t)	value	Nonparametric bootstrap Confidence Intervals
(Intercept)	-27.7588	0.1271	-218.319	<2e-16	***	
Sphingobium	-16.003	11.3858	-1.406	0.1975		-
Armatimonadetes	-10.259	3.6756	-2.791	0.0235	*	
Acidobacteria	1.1716	0.7238	1.619	0.1442		
						Quasi-Bayesian Confidence Intervals
(II)	Estimate	std. Error	t value	Pr (> t)	value	
(Intercept)	0.015315	0.004791	3.197	0.00954	**	-
Sphingobium	2.377669	0.995071	2.389	0.03799	*	

Table S4.
 List of models targeted by CMA for $\delta^{15}\text{N}$ in Fig. 6 and their statistical values. Short terms in the table mean as follows:
 ACME, average causal mediation effects; ADE, the average direct effects.

$\delta^{15}\text{N}$ regression models					(I) Delta15N ~ Gemmata + Armatimonadetes					
					(II) Gemmata ~ Fimbriimonas + Armatimonadetes					
					+ Methanobacterium + Gemmatimonadetes + Planctomycetes					
					Nonparametric bootstrap Confidence Intervals					
(I)	Estimate	std. Error	t value	Pr (> t)	value	Estimate	95% CI lower	95% CI upper	p-value	
(Intercept)	0.9237	0.4828	1.913	0.088	.	ACME	0	0	0	1
Gemmata	16.8272	28.8199	0.584	0.574		ADE	-2.92	-10.71	8.02	0.48
Armatimonadetes	14.2315	19.7173	0.722	0.489		Total Effect	-2.92	-10.71	8.02	0.48
						Prop.Mediated	0	0	0	1
					Sample Size Used :12	Simulations: 1000				
					Quasi-Bayesian Confidence Intervals					
(II)	Estimate	std. Error	t value	Pr (> t)	value	Estimate	95% CI lower	95% CI upper	p-value	
(Intercept)	0.003248	0.005729	0.567	0.5913		ACME	0	0	0	1
Fimbriimonas	3.261639	1.780156	1.832	0.1166		ADE	-2.91	-6.17	0.1	0.066
Armatimonadetes	-2.915195	1.63036	-1.788	0.124		Total Effect	-2.91	-6.17	0.1	0.066
Methanobacterium	0.380351	0.164101	2.318	0.0596		Prop.Mediated	0	0	0	1
Gemmatimonadetes	0.746686	0.387198	1.928	0.1021						
Planctomycetes	0.077369	0.05535	1.398	0.2117		Sample Size Used :12	Simulations: 1000			

Table S5.

List of models targeted by CMA for total carbon in Fig. 6 and their statistical values. Short terms in the table mean as follows: ACME, average causal mediation effects; ADE, the average direct effects.

Total C					(I)Total_C ~ Candidatus.Solibacter + Bradyrhizobium (II)Bradyrhizobium + Armatimonadetes ~ Sphingobium					
					Nonparametric bootstrap Confidence Intervals					
(I)	Estimate	std. Error	t value	Pr (> t)	value	Estimate	95% CI lower	95% CI upper	p-value	
(Intercept)	41.06	2.503	16.405	5.17E-08	***	ACME	-216.506	-7347.545	2595.02	0.812
Candidatus.Solibacter	-68.061	451.982	-0.151	0.884		ADE	-2.938	-8.985	1.92	0.286
Bradyrhizobium	193.52	260.259	0.744	0.476		Total Effect	-219.443	-7348.653	2589.88	0.814
						Prop.Mediated	0.987	0.965	1.03	0.002**
					Sample Size Used :12 Simulations: 1000					
					Quasi-Bayesian Confidence Intervals					
(II)	Estimate	std. Error	t value	Pr (> t)	value	Estimate	95% CI lower	95% CI upper	p-value	
(Intercept)	0.03413	0.01305	2.616	0.028	*	ACME	-252.719	-3544.263	2984.88	0.89
Candidatus.Solibacter	-2.93776	2.35573	-1.247	0.2438		ADE	-2.908	-7.825	1.79	0.212
Bradyrhizobium	3.18105	1.35647	2.345	0.0437	*	Total Effect	-255.627	-3547.675	2981.96	0.89
						Prop.Mediated	0.999	0.967	1.04	0.004**
					Sample Size Used :12 Simulations: 1000					

Table S6.
 List of models targeted by CMA for total nitrogen in Fig. 6 and their statistical values. Short terms in the table mean as follows: ACME, average causal mediation effects; ADE, the average direct effects.

Total N					(I) Total_N ~ Coralloccoccus + Gemmatimonas + Opitutus + Sphingobium + Devosia + Candidatus.Solibacter + Bradyrhizobium + Paenibacillus					
					(II) Devosia ~ Candidatus.Solibacter + Sphingobium					
					Nonparametric bootstrap Confidence Intervals (T: Sphingobium - M: Devosia)					
(I)	Estimate	std. Error	t value	Pr (> t)	value	Estimate	95% CI lower	95% CI upper	p-value	
(Intercept)	1.4243	0.3378	4.217	0.0244	*	ACME	0	0	0	1
Coralloccoccus	49.1327	14.6833	3.346	0.0442	*	ADE	0.79	-0.583	1.72	0.23
Gemmatimonas	83.3747	28.2376	2.953	0.0599	.	Total Effect	0.79	-0.583	1.72	0.23
Opitutus	60.682	25.6554	2.365	0.0989	.	Prop.Mediated	0	0	0	1
Sphingobium	-36.6369	26.0637	-1.406	0.2545	.	Sample Size Used :12 Simulations: 1000				
Devosia	-9.2243	16.8605	-0.547	0.6224	.	Quasi-Bayesian Confidence Intervals (T: Sphingobium - M: Devosia)				
Candidatus.Solibacter	-91.0711	37.2804	-2.443	0.0923	.	Estimate	95% CI lower	95% CI upper	p-value	
Bradyrhizobium	17.6118	24.0006	0.734	0.5162	.	ACME	0	0	0	1
Paenibacillus	51.015	16.7616	3.044	0.0557	.	ADE	0.778	-0.197	1.77	0.13
(II)	Estimate	std. Error	t value	Pr (> t)	value	Total Effect	0.778	-0.197	1.77	0.13
(Intercept)	0.008723	0.003402	2.564	0.0305	*	Prop.Mediated	0	0	0	1
Candidatus.Solibacter	-0.155179	0.387255	-0.401	0.698	.	Sample Size Used :12 Simulations: 1000				
Sphingobium	0.789838	0.502592	1.572	0.1505	.					